

EXPERT REPORT: Case No. 18 WATER 14014

for

Luca DeAngelis, Burns & McDonnell

- a) Consulted for: historical and current aquifer conditions, such as chloride transport, and modeling simulation tools
- b) The grounds for Luca DeAngelis' opinions are knowledge of pertinent information presented in City of Wichita's Response to Production Request of Equus Beds Groundwater Management District No.2 and City of Wichita's Responses to Intervener's Production Requests, as referenced in the summaries of the respective opinions below, and in several cases, excerpted and attached for convenience of reference.
- c) Luca DeAngelis' factual observations and opinions, as presented in the Proposal documents and summarized herein, include:

- i. Expert opinions based on scientific analyses:

- 2.4 Groundwater Modeling Setup - 1% Drought Simulation

Details of the USGS Equus Beds Groundwater Flow Model (EBGWM), including information regarding the model setup, calibration, sensitivity analysis and results are presented in Attachment E of the Proposal.

During use of the EBGWM for the Proposal analyses, evaluation of modeling input parameters, consideration of calibration, and confirmation of results were actively pursued by multiple personnel as a part of Burns & McDonnell Quality Control processes.

Excerpts of Attachment E pertinent to calibration are provided as Attachment A of this Report.

- 2.4.5 Streamflow - Arkansas River, Little Arkansas River, Cow Creek

Variations in river stage and flow are considered in the groundwater model using the MODFLOW-2000 stream package, and smaller streams and tributaries were simulated using the drain package.

Excerpts of Attachment E pertinent to streamflow implementation in the EBGWM are provided as Attachment B of this Report.

–

- Figure 4 - Locations of USGS Stream Gages Within and Near the ASR BSA

Major sources of aquifer recharge adjacent to the BSA are represented in the model.

- Figure 4 of the Proposal is provided as Attachment C.
- 2.4.7 Evaporation & Transpiration
 - The rate of evapotranspiration was calculated using the process set up by the USGS during development of the EBGWM.
- Excerpts of Attachment E pertinent to evaporation and transpiration implementation in the EBGWM are provided as Attachment D of this Report. Table 2-9: Groundwater Modeling Results for 1% Drought Simulation
 - This Table presents average modeled water level changes within the model at annual intervals.
 - At the end of the 8-year simulated drought, the average remaining saturated thickness as a percentage of predevelopment saturated thickness was 86% for model cells in the CWSA.
 - Table 2-9 of the Proposal has been provided as Attachment E.
- Table 2-10: Development of Proposed ASR Minimum Index Levels
 - The lowest water level, modeled or exhibited in 1993, was used as a basis for the proposed level, which reflects a proposed contingency.
 - Proposal Table 2-10 has been provided as Attachment F.
- Review and critique of the technical expert report submitted by Masih Akhbari, PhD, PE

This document is provided as Attachment G.

- d) Luca DeAngelis is a Burns & McDonnell employee; the Contracts provided in the City's Production of Documents disclose a Fee Schedule for each class of employee.
- e) Luca DeAngelis' factual observations and opinions are as presented above in this Expert Report, ASR Permit Modification Proposal, cover letter, and supporting appendices.

from the National Elevation Datum database (U.S. Geological Survey, 2009b). Wells and their associated groundwater altitudes were assigned to a model layer based on the altitude of the bottom of the well's screened interval, or, if the screened interval was unavailable, the altitude of the bottom of the well. If neither of these data values were available, then the well was not used. Hydrogeologic information stored in NWIS was used to confirm that a well was open to the *Equus* Beds aquifer. If a well was in the aquifer but was 5 or fewer ft deeper than the bottom of the modeled aquifer, the well was retained in the dataset and the water-level altitude assigned to the bottom layer of the model.

Streamflow gain or loss observation data, including a list of model cells for each stream reach and flow into or out of the aquifer along the stream reach, and time of observation were calculated and entered into the River Observation Package. Streamflow measurements at USGS streamflow gages on the Arkansas River near Maize (07143375) and Hutchinson (07143330), and on Little Arkansas River at Valley Center (07144200) and Alta Mills (07143665) (fig. 6) were used to estimate base flow (gains from and losses to the aquifer) for each model stress period when measurements from each pair of gages were available using hydrograph separation (Lim and others, 2005). Mean base flow for each stress period was calculated for each gage. Streamflow gains and losses for each stress period were then calculated by subtracting upstream gage base flow from downstream gage base flow. Streamflow gain is caused by discharge of water from the aquifer to the stream and is represented by a negative number. Conversely, streamflow loss results from water flow from the streams into the *Equus* Beds aquifer and is represented by a positive number.

Geometric Multigrid Solver

The groundwater flow equation was solved by the geometric multigrid method (Wilson and Naff, 2004), a method for solving the groundwater flow equation. Closure criteria are set to stop the iterative solver for head and flow residual. The head closure criterion was set to 0.01 ft and the flow residual criterion was set to 1,000.0 ft³/day.

Model Calibration

The groundwater-flow model was calibrated by adjusting model input data until model results matched field observations within an acceptable level of accuracy (Konikow, 1978). Both steady-state and transient hydraulic head and streamflow data were used to calibrate the model. Steady-state conditions occur when inflow to the system equals outflow from the system. Calibration to steady-state conditions was used to assess the conceptual model of groundwater flow and simulated boundary conditions, and estimate hydraulic conductivity values and recharge rates. Transient conditions occur when inflow does not equal outflow and is balanced by water flow

into or out of the aquifer from storage. Calibration to transient conditions refined the model hydraulic properties determined from the steady-state calibration and provided estimates of storage properties of the aquifer.

Calculation of parameter sensitivities was used for the steady-state predevelopment simulation to indicate the relative importance of each model input variable. Parameter values from the steady-state simulation were used as a starting point for manual calibration of the transient simulation. Hydraulic properties adjusted during the calibration process include horizontal hydraulic conductivity, vertical hydraulic conductivity between model layers, specific storage, specific yield, recharge rates, evapotranspiration, streambed hydraulic conductivity, and general head boundary conductance. After each change in one of these parameters, the simulated groundwater levels and streamflow gains and losses were compared to observed values. The difference between simulated and observed values is called the residual. Parameter estimation (Harbaugh and others, 2000) was attempted for the transient simulation; however, nonconvergence for the transient parameter-estimation simulations prevented its use. The nonconvergence was most likely caused by nonlinear groundwater flow, heterogeneous hydraulic properties of the *Equus* Beds aquifer, and complexity of the transient simulation.

The model accuracy was estimated using several methods. The root mean square (RMS) error between observed and simulated hydraulic head as well as observed and simulated streamflow gains or losses were calculated for each well and stream observation for the entire simulation. Model accuracy was increased by minimizing the RMS error during the calibration process. The RMS error measures the absolute value of the variation between measured and simulated hydraulic heads at control points or the variation between measured and simulated streamflow along stream reaches. The equation to calculate the RMS error is:

$$\text{RMS error} = \sqrt{\frac{e_1^2 + e_2^2 + e_3^2 + \dots + e_n^2}{n}}, \quad (5)$$

where

- e is the difference between the observed and simulated values, and
- n is the number of observations.

Water-table altitudes range from about 1,500 to about 1,300 ft above NAVD 88 in the main part of the model area between Hutchinson and Wichita, Kans. (or 200 ft of head loss, excluding the dune sand area) (Myers and others, 1996). The ratio of the RMS error to the total head loss in the model area is a measure of the amount of model error in the overall model response. A value less than 10 percent is a generally accepted threshold (Anderson and Woessner, 1992). Thus, for this study, the RMS error divided by the total head loss should be less than 20 ft (10 percent of the 200 ft of head loss in the model area).

The mean error between observed and simulated hydraulic head and between observed and simulated streamflow gains

and losses was calculated for each well and each stream observation for the entire simulation. In keeping with the MODFLOW-2000 convention, simulated results were subtracted from observed values. Negative errors indicated the simulated results were too large (simulated result needs to decrease), positive errors indicated the simulated results were too small (simulated result needs to increase). Model accuracy increased the closer the value of the mean error was to zero. The mean error measured the average difference between measured and simulated hydraulic heads at control points or the variation between measured and simulated streamflow gains and losses along stream reaches, and indicated if simulated results were higher or lower than measured observations.

The accuracy of water-level measurements also was one of the criteria used to assess values of the RMS and mean errors used to determine if the model calibration was acceptable. Most groundwater levels used for calibration were measured with a steel tape or an electric water-level measuring tape to the nearest 0.01 ft. Historical water levels for wells were measured or estimated using unknown techniques. For these water-level measurements, the accuracy is assumed to be within 1 ft. The measuring-point altitudes for most wells used in this study were obtained using standard surveying or global positioning system methods. The accuracy of these altitudes is between 0.01 and 0.5 ft. The measuring-point altitude of a few wells in the study area was estimated from USGS 7.5-minute topographic maps. The vertical accuracy of land-surface altitudes from these maps is one-half of the contour interval. The contour interval on topographic maps is 5 or 10 ft and the accuracy of measuring-point altitudes for these wells is 2.5 or 5 ft, respectively; therefore, the largest possible error in measurement of water-level altitudes is approximately 5 ft.

Water levels measured in monitoring wells located near pumping wells are closely related to the rate of pumping. The use of an average pumping rate instead of the actual pumping rate can introduce substantial error between a simulated and measured water level. The most likely instance when this would occur is when average annual pumping rates are used. Typical well-field pumping consists of increasing and decreasing pumping rates by turning wells on or off to meet water-supply demand. If the water level was measured when the nearby well was pumping, the simulated water levels will be greater than the measured water level. If the well was not pumping, the simulated water levels will be too low. This type of error is not quantified easily but could be several feet if the measured well is close to the pumping well. The maximum possible error for water-level measurements is the sum of the maximum errors caused by water-level measurement errors, measuring-point altitude errors, and well pumping. The chance that the maximum error would occur at any well is small. A combination of errors of varying value and sign is more likely to occur.

River stage is measured at USGS streamflow gages to the nearest 0.01 ft. Streamflow measurement accuracy is plus or minus 2 percent of the actual value for “excellent” measurements, plus or minus 5 percent for “good” measurements, and

plus or minus 8 percent for “fair” measurements (Rantz and others, 1982). An estimate of the error associated with the calculation of base flow was made using the assumption that all streamflow measurements were “good” and each measurement was within 5 percent of the actual value. Estimated base flow for each gage was multiplied by 0.05 to obtain an estimate of the error in base flow from the error in each streamflow measurement. The largest base flow error from measurement is represented by two conditions, subtracting a high upstream measurement from a low downstream measurement, and subtracting a low upstream measurement from a high downstream measurement. These two conditions were used to calculate the largest and smallest measurement error for estimated base flow observations. For the Arkansas River streamflow gain or loss observations the largest estimated base flow error from streamflow measurements is almost 12,375,000 ft³/day (143 ft³/s), the smallest is almost 556,000 ft³/day (6 ft³/s), and the mean is almost 3,615,000 ft³/day (42 ft³/s). For the Little Arkansas River estimated base flow observations, the largest estimated base flow error from measurements is more than 4,300,000 ft³/day (50 ft³/s), the smallest is more than 132,000 ft³/day (2 ft³/s), and the mean is almost 1,088,000 ft³/day (13 ft³/s).

The amount of error associated with the method used to estimate base flow is unknown but may be substantial. Estimates of base flow may be affected by streamflows that result from regulation. These may include flows from sewage treatment facilities, flood control reservoirs, and water-supply diversions. Also, base flow estimates are related to the hydrologic conditions of the period of record used in the analysis. Base flow estimated during a dry or wet period will be biased toward those conditions (Sloto and Crouse, 1996). Knowledge of errors associated with observation data is important for choosing an appropriate calibration target and for preventing calibration of the model to an error substantially smaller than the errors associated with the measurement of the observed data.

For the Arkansas River, estimated base flow observations near Maize (07143375) at river mile 772.2 ranged from almost 4,370,000 to almost 139,290,000 ft³/day (51 to 1,612 ft³/s), and at Hutchinson (07143330) at river mile 800.3 from more than 6,655,000 to more than 108,193,000 ft³/day (77 to 1,252 ft³/s). Observed base flow was calculated for each reach and for all base flow observations, and the minimum was subtracted from the maximum to calculate the range of observed base flow. The range of observed base flow on the Arkansas River between Maize (07143375) and Hutchinson (07143330), 28.1 river miles in length was 35,778,000 ft³/day (414 ft³/s). For the Little Arkansas River, estimated base flow observations at Valley Center (07144200) at river mile 17.5 ranged from more than 2,052,000 to more than 56,528,000 ft³/day (24 to 654 ft³/s), and at Alta Mills (07143665) at river mile 50.1 from more than 473,000 to more than 29,700,000 ft³/day (5 to 344 ft³/s). The range of observed base flow on the Little Arkansas River between Valley Center and Alta Mills, 32.6 river miles in length was almost 25,371,000 ft³/day (294 ft³/s). The ratio of the RMS error to the total range in observed base flow is a

measure of the amount of base flow error in the overall model response. Accounting for errors in base flow from streamflow measurements and errors associated with base flow estimation using hydrograph separation, an arbitrary value of 25 percent was chosen as an acceptable ratio of RMS error for simulated base flow to total range in estimated base flow. The RMS error to total range in observed base flow should be less than 8,944,500 ft³/day (103.5 ft³/s) for the Arkansas River and less than 6,342,750 ft³/day (73.4 ft³/s) for the Little Arkansas River.

Steady-State Calibration

The steady-state hydraulic head data were obtained from historic groundwater level data from 284 wells in the study area. Well locations are shown in figure 32 and the well number, date of observation, observed water level, and simulated water level of each well used in the steady-state calibration are listed in table 7 at the back of this report. Head observation data were collected between 1935 and 1939. Concurrent streamflow measurements between gage pairs are unavailable for the Arkansas and Little Arkansas Rivers before 1959, thus the steady-state simulation could not be calibrated to streamflow gains or losses. Values for river stage, recharge, evapotranspiration, and well pumping averaged from 1935 to 1939 were assumed to approximate steady-state conditions. In reality, river stage, recharge, evapotranspiration, and well pumping were variable during this time and groundwater levels responded to these changes. Because the amount of well pumping was relatively small and constant, and groundwater level and river stage measurements from one gage each on the Arkansas and Little Arkansas Rivers are available, this period is the best estimation of pre-development conditions for model calibration. The RMS error for the steady-state calibration simulation is 9.82 ft. The ratio of the RMS error to the total head loss in the model area is 0.049 (9.82 ft divided by 200 ft) or 4.9 percent. The level of accuracy of the simulation in representing the steady-state hydraulic-head distribution was acceptable because it is less than 10 percent of the change in groundwater level across the model, and is close to the assumed groundwater level measurement errors previously discussed. The mean error (observed–simulated) for 284 water-level observations is 3.86 ft.

The location of wells and calibration residuals calculated as the simulated head minus observed head in ft at each well with an observation is shown in figure 32. For most of the modeled area, simulated head is within 5 ft of observed head. Simulated heads are more than 5 ft greater than observed heads near the Wichita well field. The larger simulated heads are assumed to be the result of observations recorded in 1939 when well pumping was larger but simulated pumping was lower because pumping was averaged from 1935 through 1939. The observed and simulated groundwater level maps from 1940 are shown in figure 33.

Steady-State Groundwater Flow Budget

Inflows and outflows to the groundwater model were recorded for the steady-state calibration simulation and are listed in table 8. Total simulated flow through the groundwater system was more than 49 million ft³/day. Major inflows to the system as a percent of total flow were recharge (64.7 percent) and river leakage (30.5 percent). Major outflows from the system were river leakage (51.8 percent), evapotranspiration (38.8 percent), drains (4.6 percent), and well pumping (4.6 percent). The difference between inflows and outflows, called the mass balance, indicates the ability of the numerical model to solve the groundwater flow equation such that numerical errors are small. The difference between flows into and out of the model was -0.08 percent of total flow for the steady-state calibration simulation.

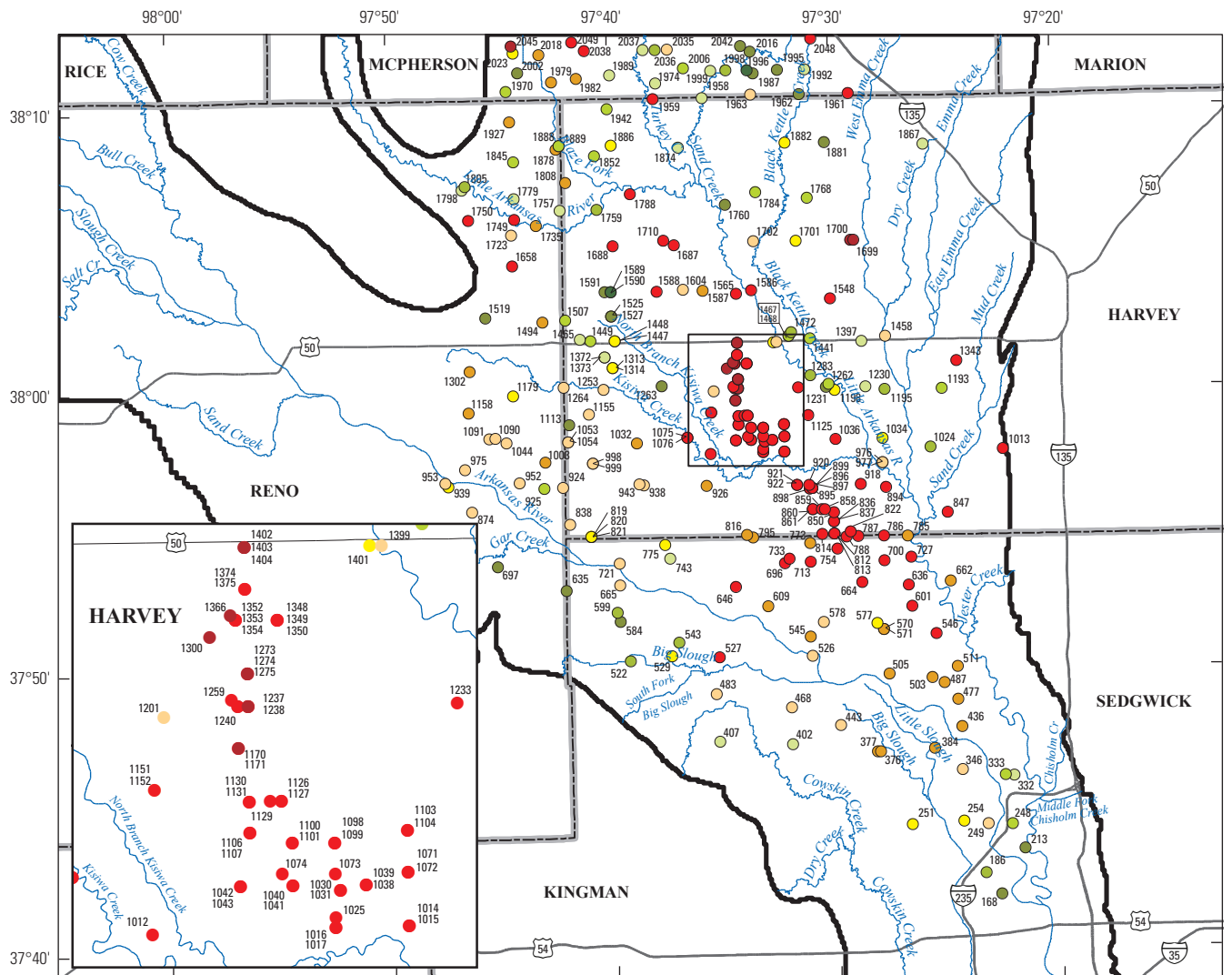
Transient Calibration

Hydraulic-head data for the transient calibration were obtained from 346 wells in the study area (fig. 34). The well number, date of observation, observed water level, and simulated water level for each well used in the transient calibration are listed in table 9 at the back of this report. Wells were selected to include all model layers and a wide distribution in the model. A total of 3,677 water-level observations from 1935 through 2008 were used for the transient calibration. The RMS error for all water-level observations is 2.48 ft for the transient calibration. This value is less than the maximum measurement errors and indicates the acceptability of the calibrated model. The ratio of the RMS error to the total head loss in the model area (2.48/200) is 0.0124, or 1.24 percent. The mean error for all water level observation wells used in the transient calibration is 0.03 ft.

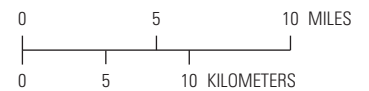
Table 8. Steady-state calibration simulation flow budget.

[ft³/day, cubic feet per day; acre-ft/day, acre feet per day; --, not applicable]

Budget component	Flow rate, in ft ³ /day	Flow rate, in acre-ft/day	Percent of total flow
Inflow			
Head dependent boundaries	2,320,409	53.3	4.7
Recharge	31,855,858	731.3	64.7
River leakage	15,024,649	344.9	30.5
Well pumping	0	0.0	0.0
Total in	49,200,916	1,129.5	100
Outflow			
Head dependent boundaries	1,167,715	26.8	0.2
Evapotranspiration	18,569,682	426.3	38.8
Drains	2,129,863	48.9	4.6
River leakage	25,165,966	577.7	51.8
Well pumping	2,204,735	50.6	4.6
Total out	49,237,960	1,130.3	100
Total in - out	37,044	0.9	--
Percent difference	-0.08	-0.08	--



Base from U.S. Geological Survey digital data, 2005, 1:100,000
 Universal Transverse Mercator projection
 Zone 14



EXPLANATION

- Active model boundary
- 251 Monitoring well and number—Simulated head minus observed head, in feet
- -36.8 to -20.0
- -19.9 to -5.0
- -4.9 to -3.0
- -2.9 to -1.0
- -0.9 to 0.0
- 0.1 to 1.0
- 1.1 to 3.0
- 3.1 to 5.0
- 5.1 to 20.0
- 20.1 to 48.7

Figure 32. Monitoring well locations and residuals (simulated head minus observed head, in feet) for the steady-state calibration simulation.

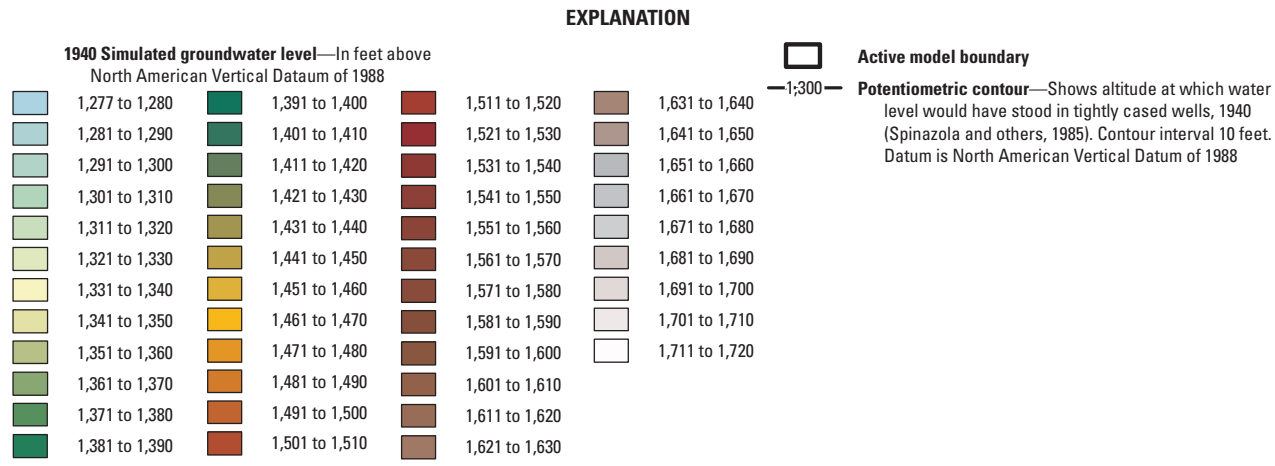
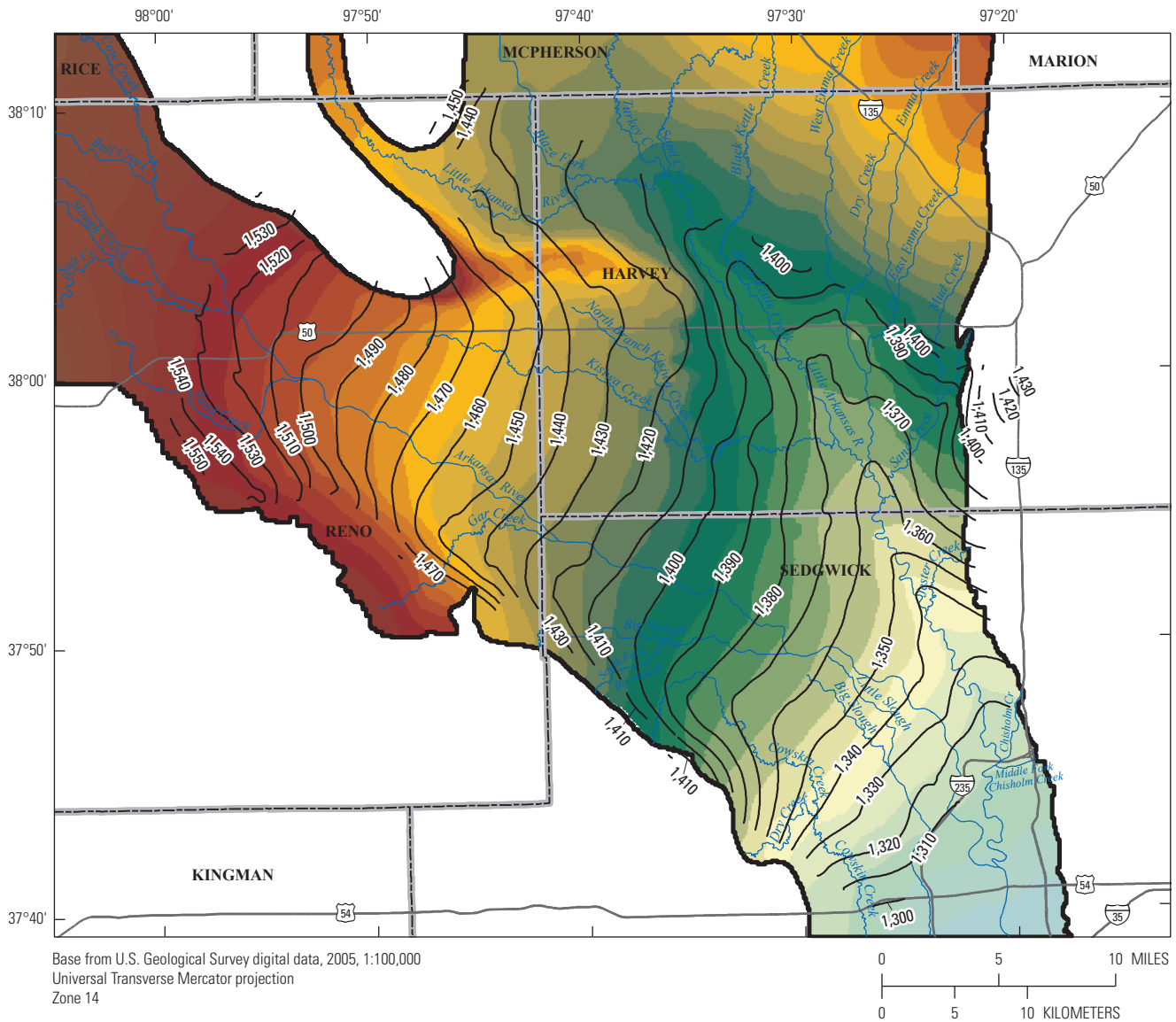


Figure 33. Observed and simulated *Equus* Beds aquifer groundwater levels, 1940.

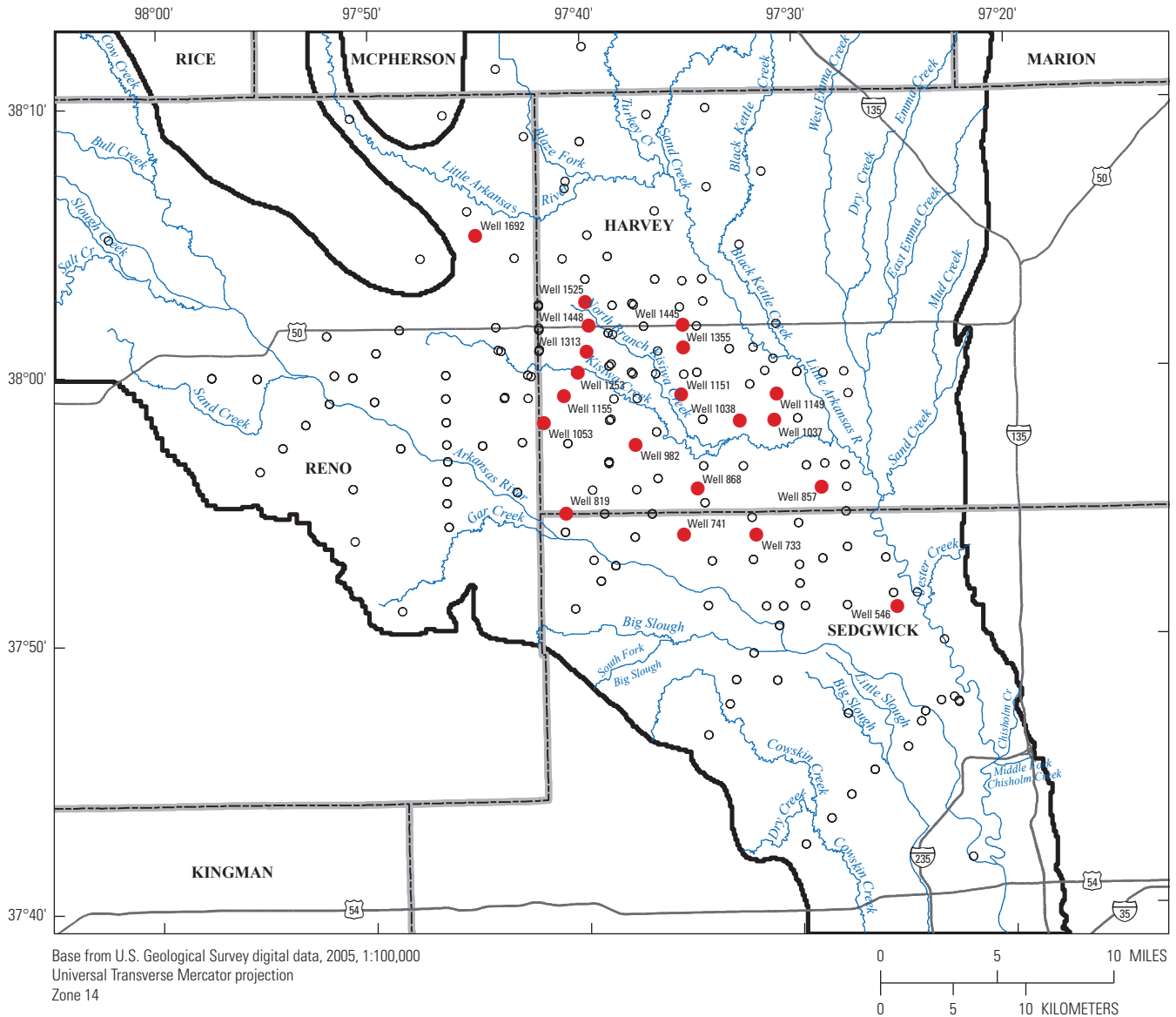


Figure 34. Monitoring well locations used for the transient calibration simulation.

Simulated versus observed groundwater levels closely match the one to one line and are plotted in figure 35. The modeled area was divided into six zones (fig. 36) with calibration statistics calculated for each zone to allow assessment of model calibration for different model areas. Zone 1 is the basin storage area and contains the index wells and artificial-recharge accounting index cells (used by the city to monitor water levels in the aquifer and any changes that might occur as a result of the ASR project, fig. 3), zone 2 is near the Burrton area, zone 3 is near the Arkansas River, zone 4 is the dune sand area, zone 5 is the upland area south of the Arkansas River, and zone 6 is the upland area north and east of the Little Arkansas River. These zones roughly correspond to similar zones presented in Myers and others, (1996), except for zone 4. Calibration zones, RMS error, the RMS error divided by the head loss, and mean error for each calibration zone are listed in table 10. Monitoring well locations used for calibration in the transient simulation are indicated by zone on figure 36.

The areal distribution of mean error, the average difference between observed and simulated groundwater levels for all wells and for the entire transient simulation period, can reveal areas of the model that consistently over- or under-simulate groundwater levels. The mean error for wells in each model layer is shown in figures 37, 38, and 39. The distribution of mean error for simulated groundwater levels in model layer 1 does not indicate a spatial bias in most of the modeled area (fig. 37). In the area south of the Arkansas River, near Mount Hope (fig 1), simulated groundwater altitudes are greater than observed and simulated groundwater altitudes are less than observed in the dune sand area north of Burrton. For model layer 2, simulated groundwater altitudes are slightly less than observed to the southwest of Burrton and along the Arkansas River between Hutchinson to just upstream from Mount Hope (fig. 38). No spatial bias in mean error is apparent for the rest of model layer 2. The distribution of mean error for model layer 3 (fig. 39) indicates simulated groundwater altitudes are slightly less than observed to the southwest of Burrton and along the Arkansas River between Hutchinson to just upstream from Mount Hope, as was indicated in model

layer 2. North of the Little Arkansas River, between Blaze Fork and Turkey Creek simulated groundwater altitudes are greater than observed in layer 2.

Comparison of simulated and observed well hydrographs is used to assess the response of simulated groundwater levels to temporal changes in stresses to the aquifer. Simulated and observed groundwater levels are shown for 20 selected wells in figure 40. Multiyear stress periods were simulated from 1935 through 1989 and annual stress periods were simulated from 1990 through 2008. Multiyear trends in the hydrographs are illustrated by the overall trends from 1935 through 2008. Simulated water levels follow the observed long-term trends for most wells, indicating the model adequately simulates long-term changes to groundwater levels resulting from sustained stresses on the aquifer such as long-term rate of groundwater withdrawal, gains from and losses to streams, or long-term trends in recharge.

Some differences in long-term trends are apparent in the simulated versus observed hydrographs for wells 733, 741, 819, 868, 1053, 1149, 1155, 1253, and 1525 in the multiyear stress period for 1953 through 1958 (fig. 40). All of these wells show simulated water levels went down or the rate of decrease was faster during the 1950s but the observed water levels went up or the rate of decrease was slower. The most likely explanation for this is that average rainfall assigned to the 1953 to 1958 stress period is less than during 1958 when observed groundwater levels were measured. Average rainfall for the 1953–58 stress period was about 25 inches per year; however, in 1957, rainfall was almost 40 inches per year and in 1958 rainfall was almost 36 inches per year (fig. 25). The lower simulated values were caused by using the average rainfall rate for the stress period. The larger observed values resulted from water levels that were used as observations and measured in 1958 after they had increased in response to the larger than average rainfall for 1957 and 1958.

Annual trends are illustrated in the hydrographs between 1990 and 2008 when annual pumping, annual stream flow, and annual recharge were simulated. Simulated short-term trends follow observed water level trends for most wells. Differences between annual simulated and observed water levels are most

Table 10. Root Mean Square error, the ratio of Root Mean Square error to head loss, and mean error for each transient calibration zone.

[--, not applicable]

Calibration zone	Calibration zone from Myers and others (1996)	Root mean square error, in feet	Ratio of root mean square error to head loss, in feet	Mean error, in feet (negative value indicates simulated is larger than observed)	Mean absolute difference (Myers and others, 1996)
1 (Basin Storage Area)	5	2.74	0.014	-0.199	6.76
2 (Burrton Area)	1	2.45	0.012	-0.055	5.76
3 (Arkansas River)	2	1.5	0.008	0.518	2.47
4 (Sand Dunes)	--	2.09	0.01	1.58	--
5 (South Uplands)	3	1.39	0.007	0.167	2.15
6 (North Uplands)	4	8.35	0.042	-6.258	6.76

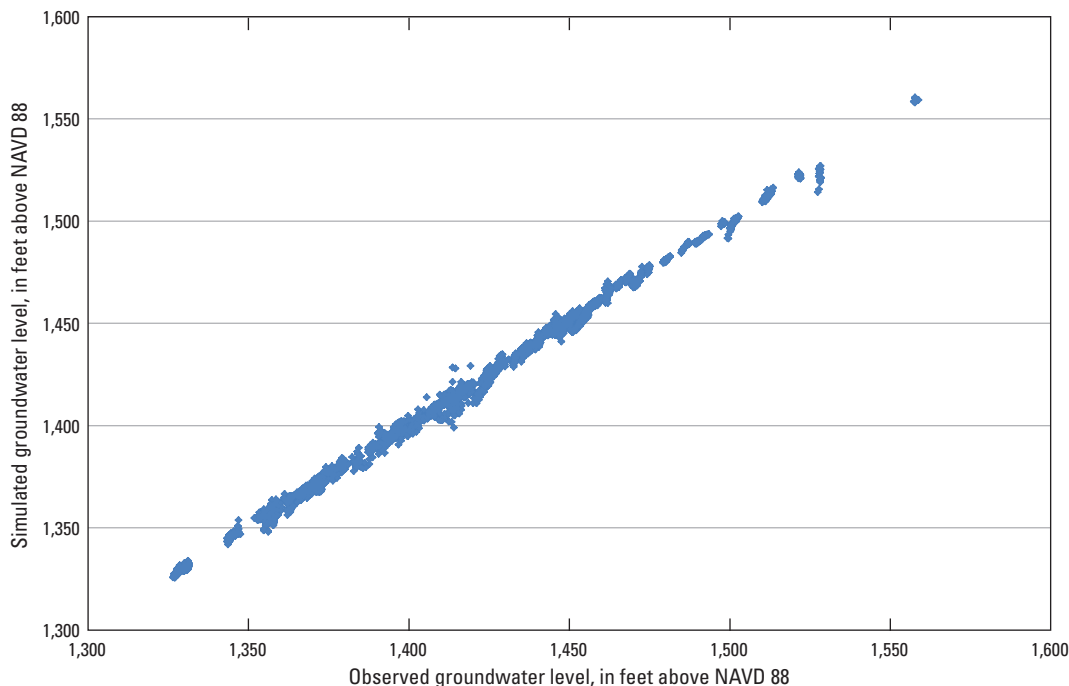


Figure 35. Simulated versus observed groundwater levels for the transient calibration.

apparent for wells 857, 868, 1448, and 1692 (fig. 40), where large short-term variations in the observed water levels are not well simulated although the overall trends are similar. These differences between simulated and observed short-term water levels for wells are most likely caused by observed water levels measured after large stresses such as precipitation events that occur in a shorter time interval than the model stress periods or heterogeneities in the hydraulic properties of the aquifer at these locations that are not incorporated into the model.

The RMS error calculated for observed and simulated base flow gains or losses for the Arkansas River for the transient simulation was 7,916,564 ft³/day (91.6 ft³/s) and the RMS error divided by the total range in streamflow (7,916,564/37,461,669 ft³/day) is 22 percent. The RMS error calculated for observed and simulated streamflow gains or losses for the Little Arkansas River for the transient simulation was 5,610,089 ft³/day (64.9 ft³/s) and the RMS error divided by the total range in streamflow (5,612,918/41,791,091 ft³/day) is 13 percent. The RMS values are less than the maximum measurement errors and the RMS error divided by the total range in streamflow are less than 25 percent, indicating the acceptability of the simulated streamflow gains or losses in the transient calibrated model. The mean error between observed and simulated base flow gains or losses was 29,999 ft³/day (0.34 ft³/s) for the Arkansas River and -1,369,250 ft³/day (-15.8 ft³/s) for the Little Arkansas River. Observed and simulated streamflow gains or losses for each stress period are listed in table 11 at the back of this report. Comparison of observed and simulated cumulative streamflow gains or losses indicate how well the model simulates long-term streamflow

gains or losses. Cumulative streamflow gain and loss observations are similar to the cumulative simulated equivalents and are shown for the Arkansas River and Little Arkansas River in figure 41.

Transient Groundwater Flow Budget

Inflows and outflows to the groundwater model were recorded for each stress period of the transient simulation. Average flow rates and cumulative flows for the transient calibration simulation are listed for each stress period in table 12 at the back of the report. Cumulative inflows to the system as a percent of total flow from largest to smallest were recharge (67 percent), river leakage (27 percent), head-dependent boundaries (4 percent), and storage (2 percent). Cumulative outflows from the system from largest to smallest were river leakage (42 percent), evapotranspiration (34 percent), well pumping (16 percent), drains (4 percent), storage (2 percent), and head-dependent boundaries (2 percent). Average percent mass balance difference for individual stress periods ranged from -0.46 to 0.51 percent. The cumulative mass balance for the transient calibration was 0.01 percent.

Parameter Sensitivity

A sensitivity analysis was performed to assess the response of the model to changes in various input parameter values. When the model is sensitive to an input parameter, small changes to the parameter value cause large changes in hydraulic head. If a change of parameter value does not change the simulated hydraulic head distribution, the model is

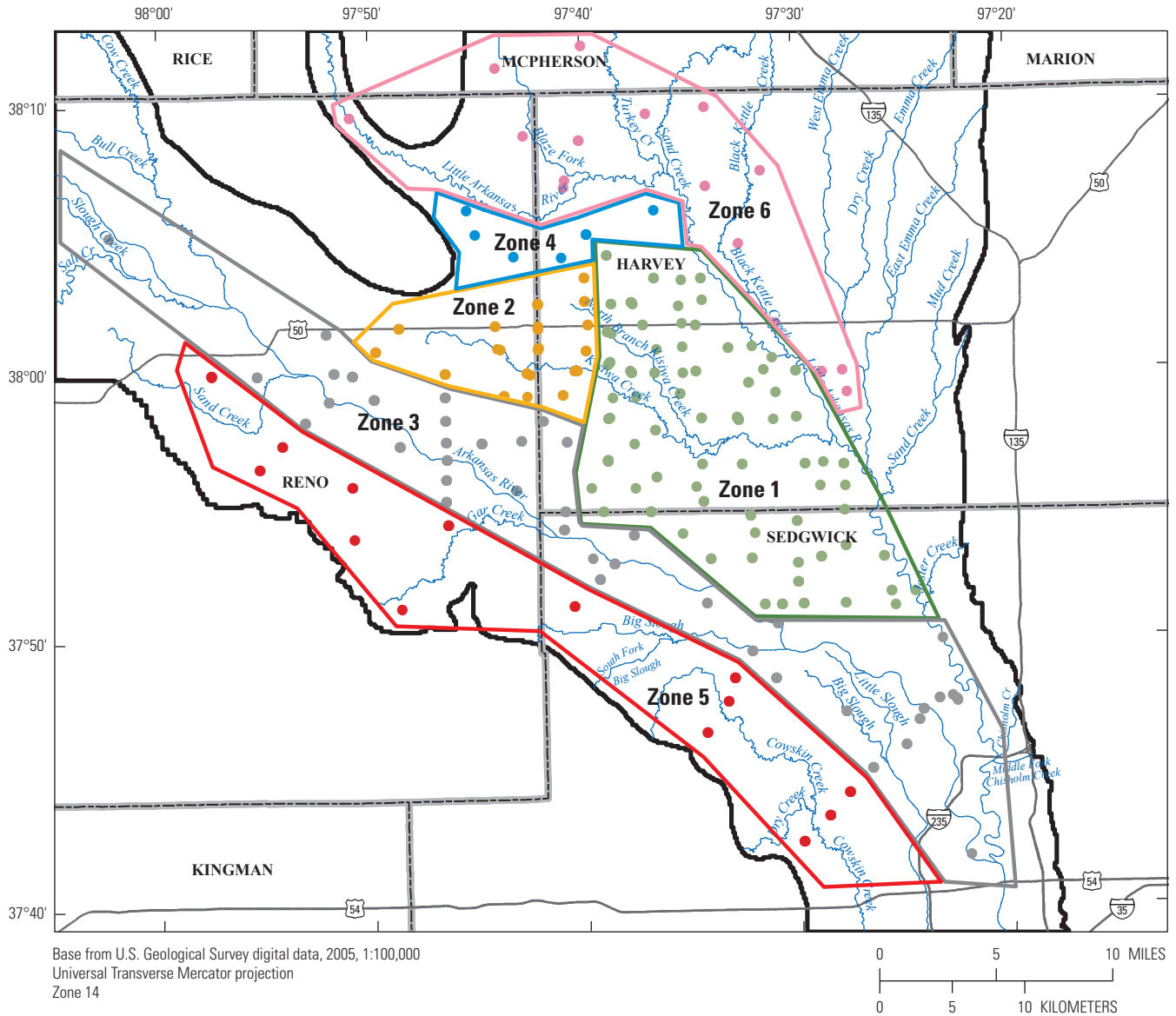
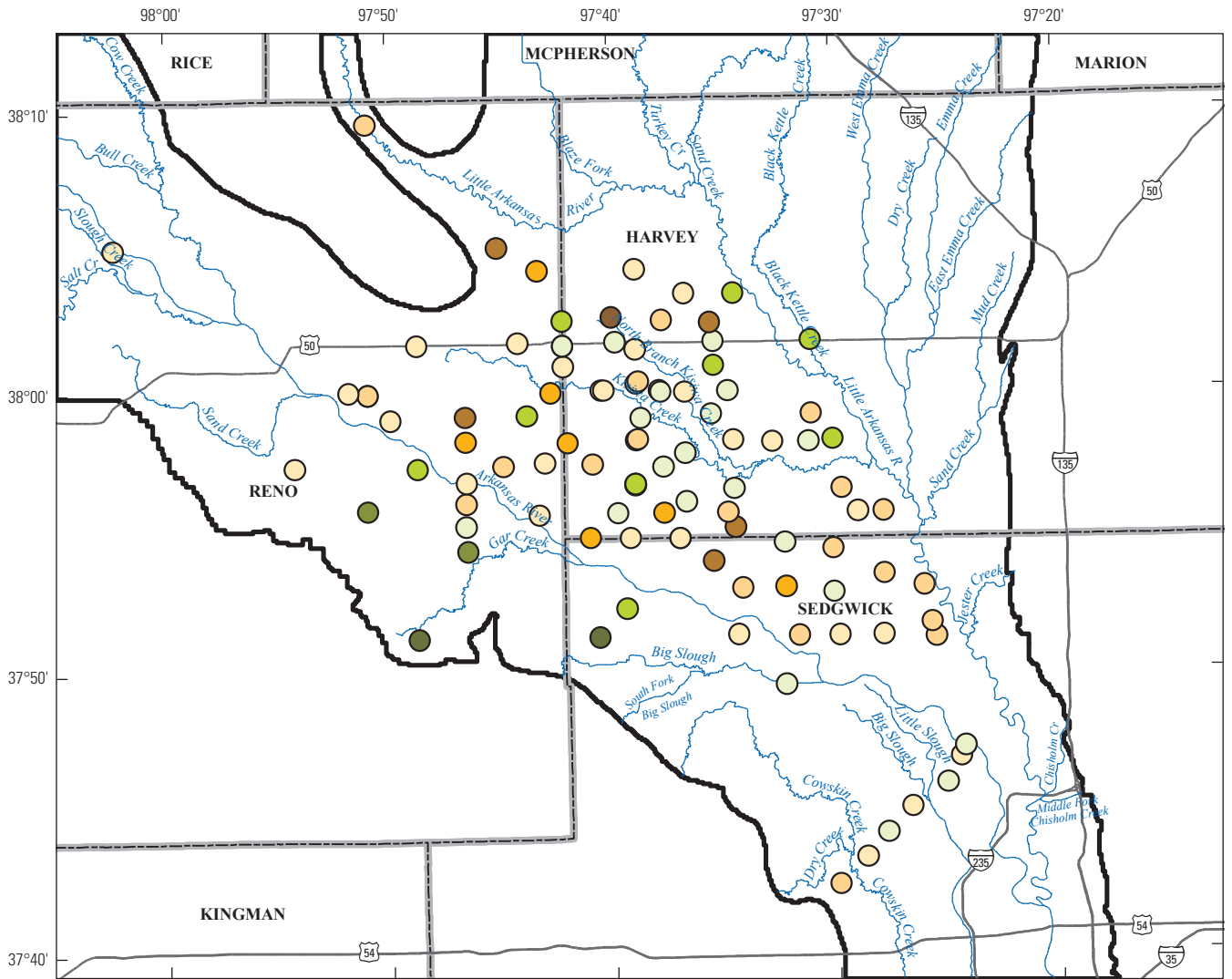
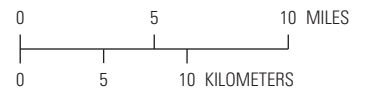


Figure 36. Calibration zones for monitoring wells used for calibration in the transient simulation.



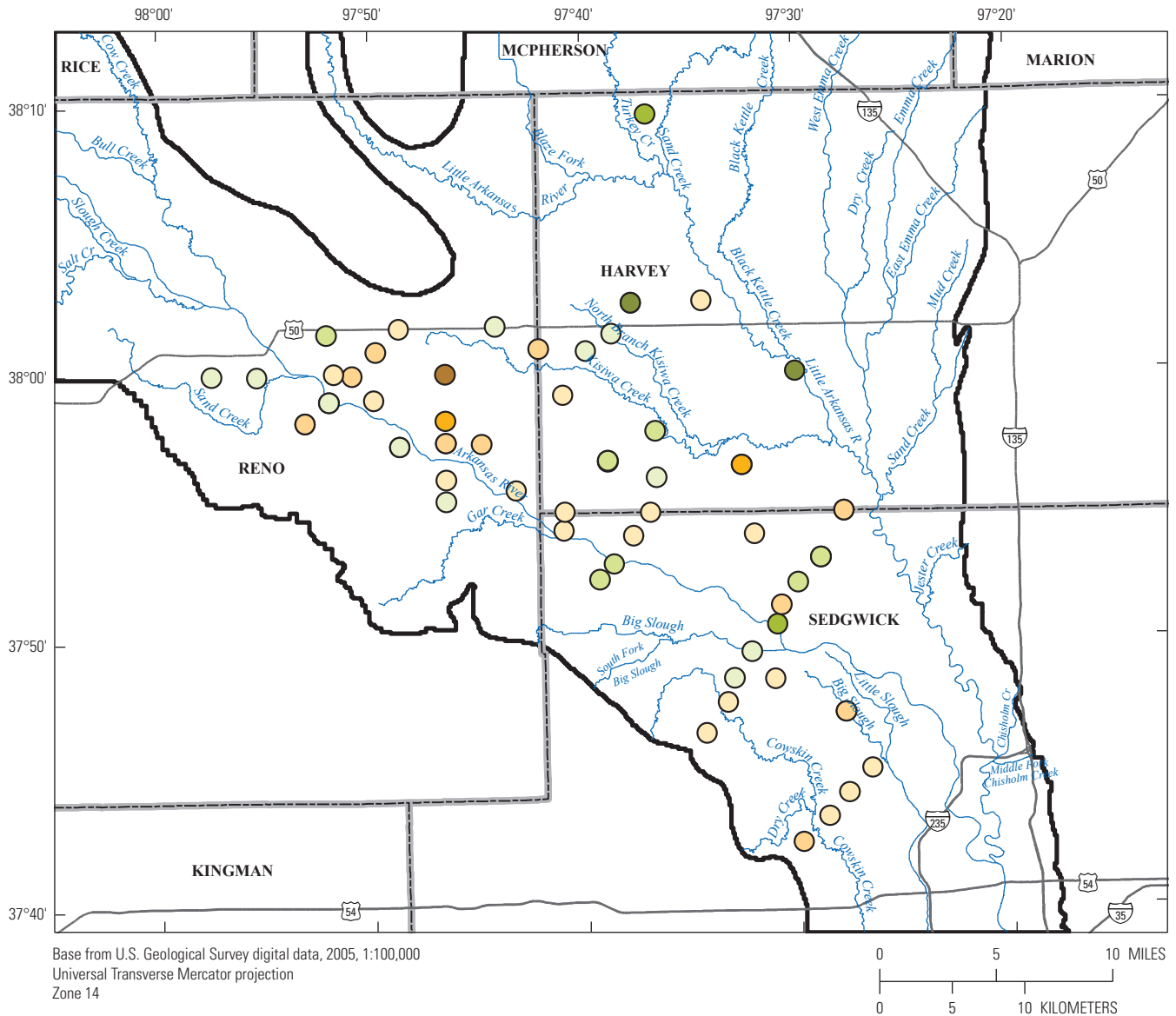
Base from U.S. Geological Survey digital data, 2005, 1:100,000
 Universal Transverse Mercator projection
 Zone 14



EXPLANATION

- Active model boundary
- Mean error model layer 1
simulated minus
observed—In feet**
- 7.4 to -5.0
- 4.9 to -3.0
- 2.9 to -2.0
- 1.9 to -1.0
- 0.9 to 0.0
- 0.1 to 1.0
- 1.1 to 2.0
- 2.1 to 3.0
- 3.1 to 5.0
- 5.1 to 5.0

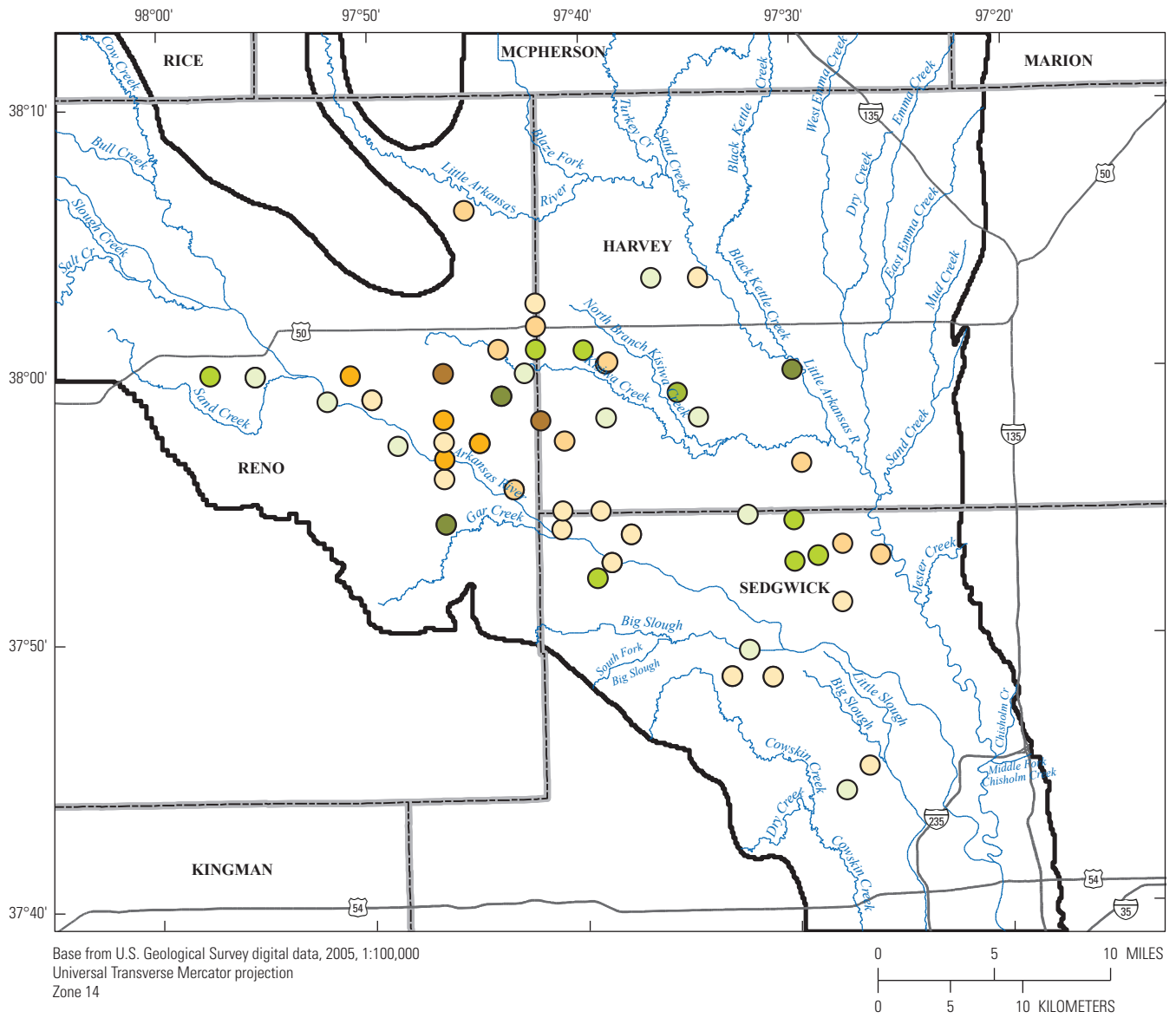
Figure 37. Mean error between observed and simulated water levels from wells in model layer 1 for the transient calibration period.



EXPLANATION

- Active model boundary**
- Mean error model layer 2 simulated minus observed—In feet**
- 4.7 to -3.0
- 2.9 to -2.0
- 1.9 to -1.0
- 0.9 to 0.0
- 0.1 to 1.0
- 1.1 to 2.0
- 2.1 to 3.0
- 3.1 to 3.7

Figure 38. Mean error between observed and simulated water levels from wells in model layer 2 for the transient calibration period.



EXPLANATION

Active model boundary

Mean error model layer 3 simulated minus observed—In feet

●	-6.7 to -5.0	●	0.1 to 1.0
●	-4.9 to -3.0	●	1.1 to 2.0
●	-2.9 to -2.0	●	2.1 to 3.0
●	-1.9 to -1.0	●	3.1 to 3.6
●	-0.9 to 0.0		

Figure 39. Mean error between observed and simulated water levels from wells in model layer 3 for the transient calibration period.

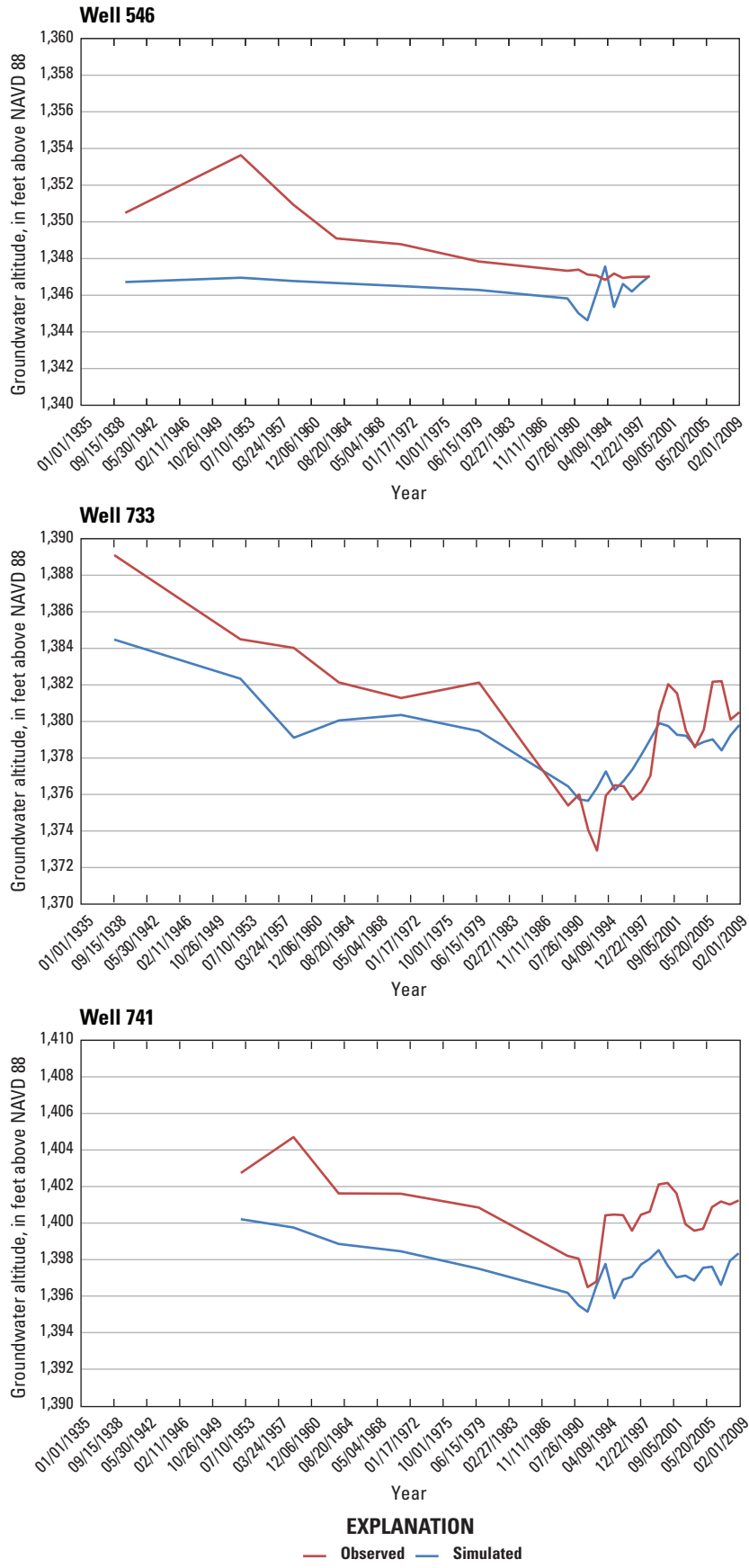


Figure 40. Simulated and observed groundwater levels for selected wells.

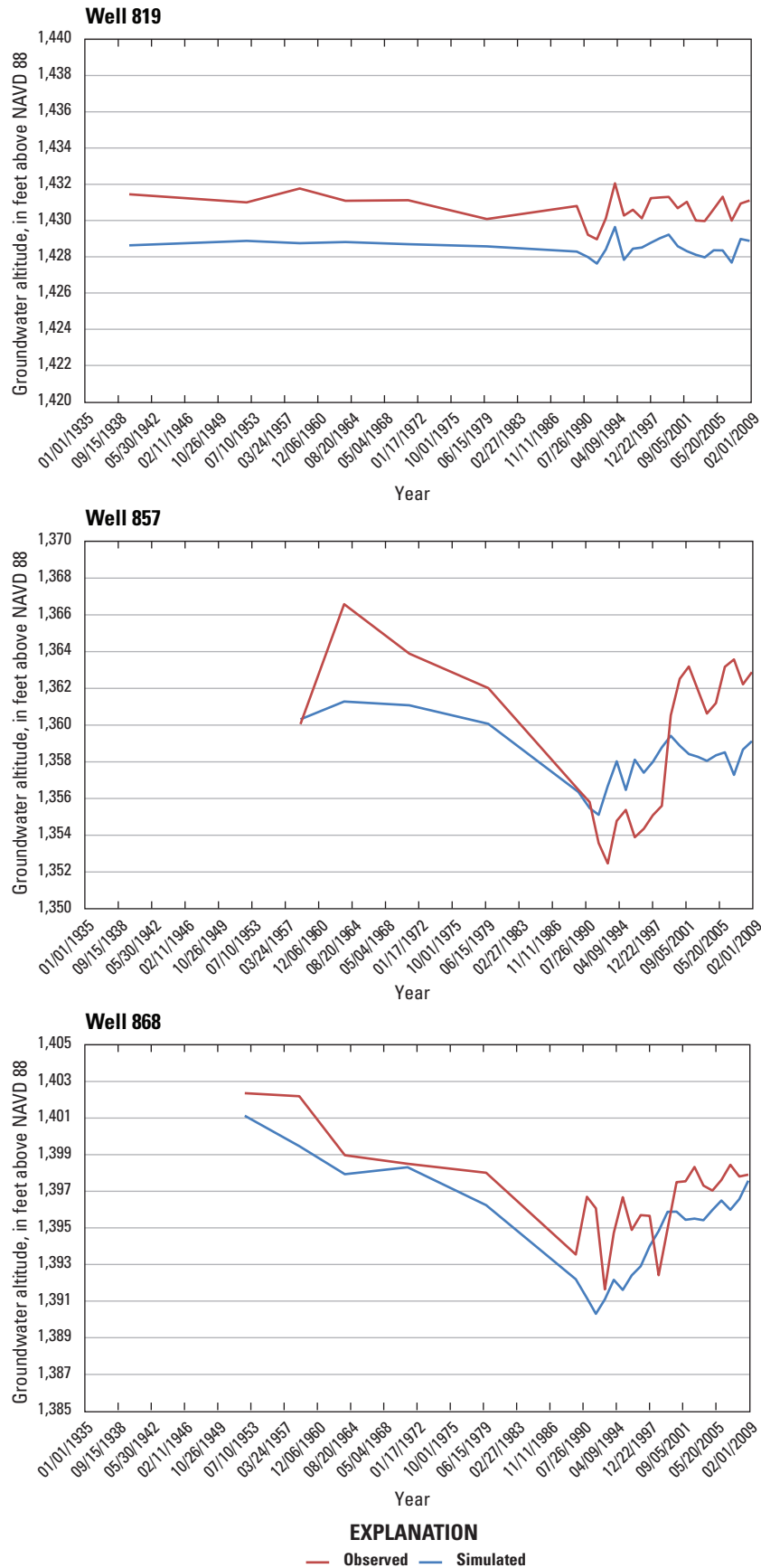


Figure 40. Simulated and observed groundwater levels for selected wells.—
Continued

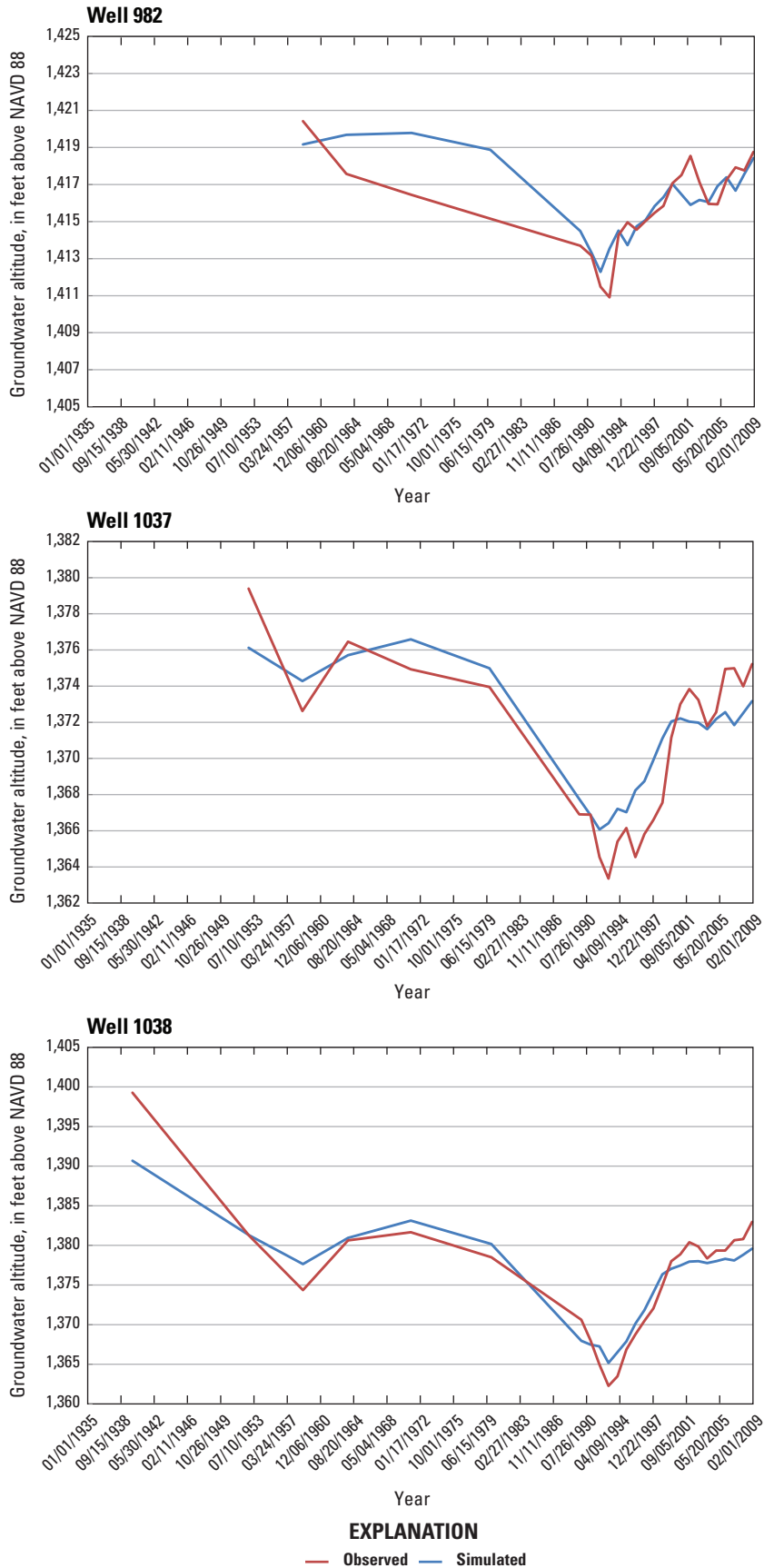


Figure 40. Simulated and observed groundwater levels for selected wells.—
Continued

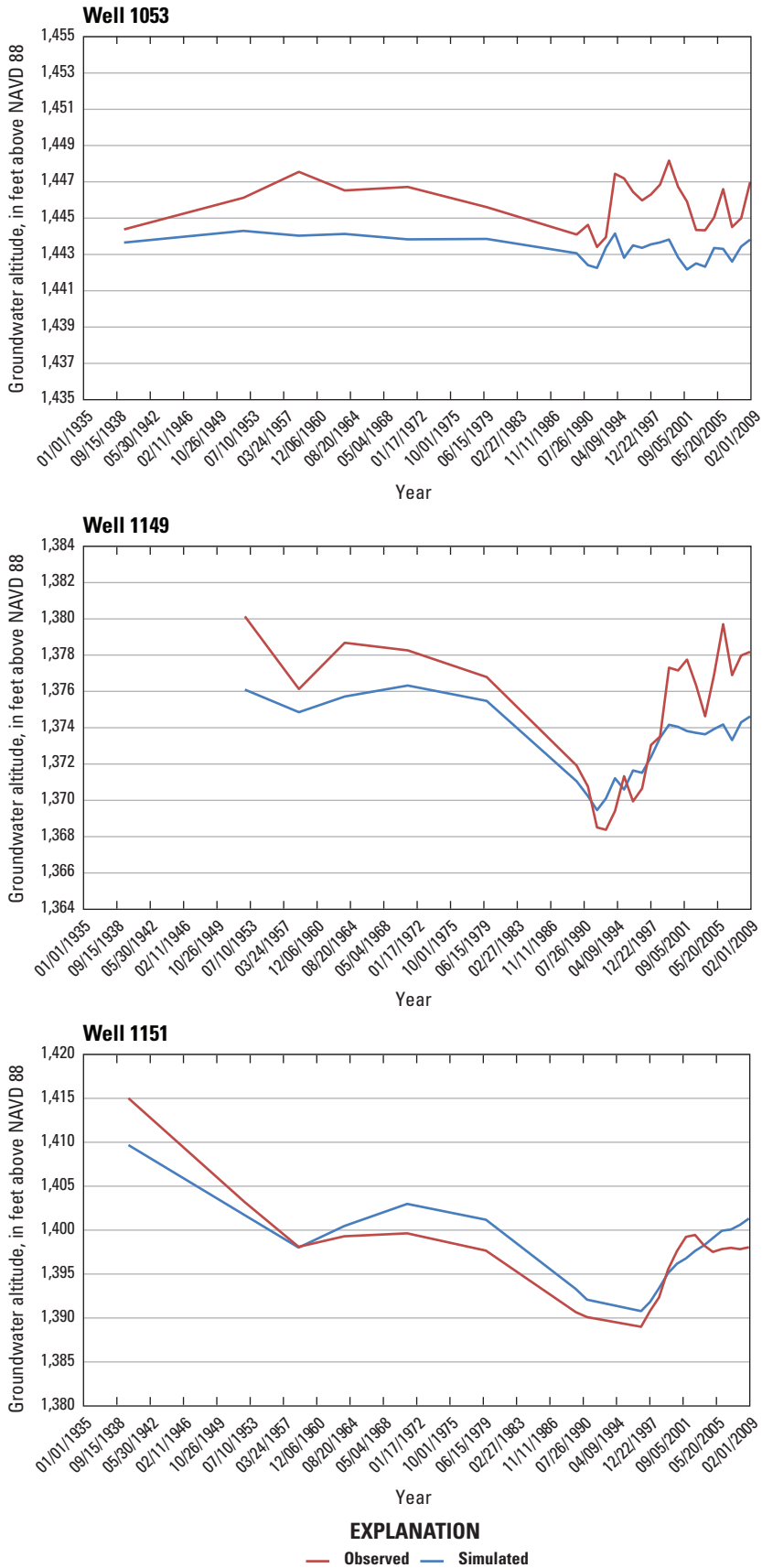


Figure 40. Simulated and observed groundwater levels for selected wells.—
Continued

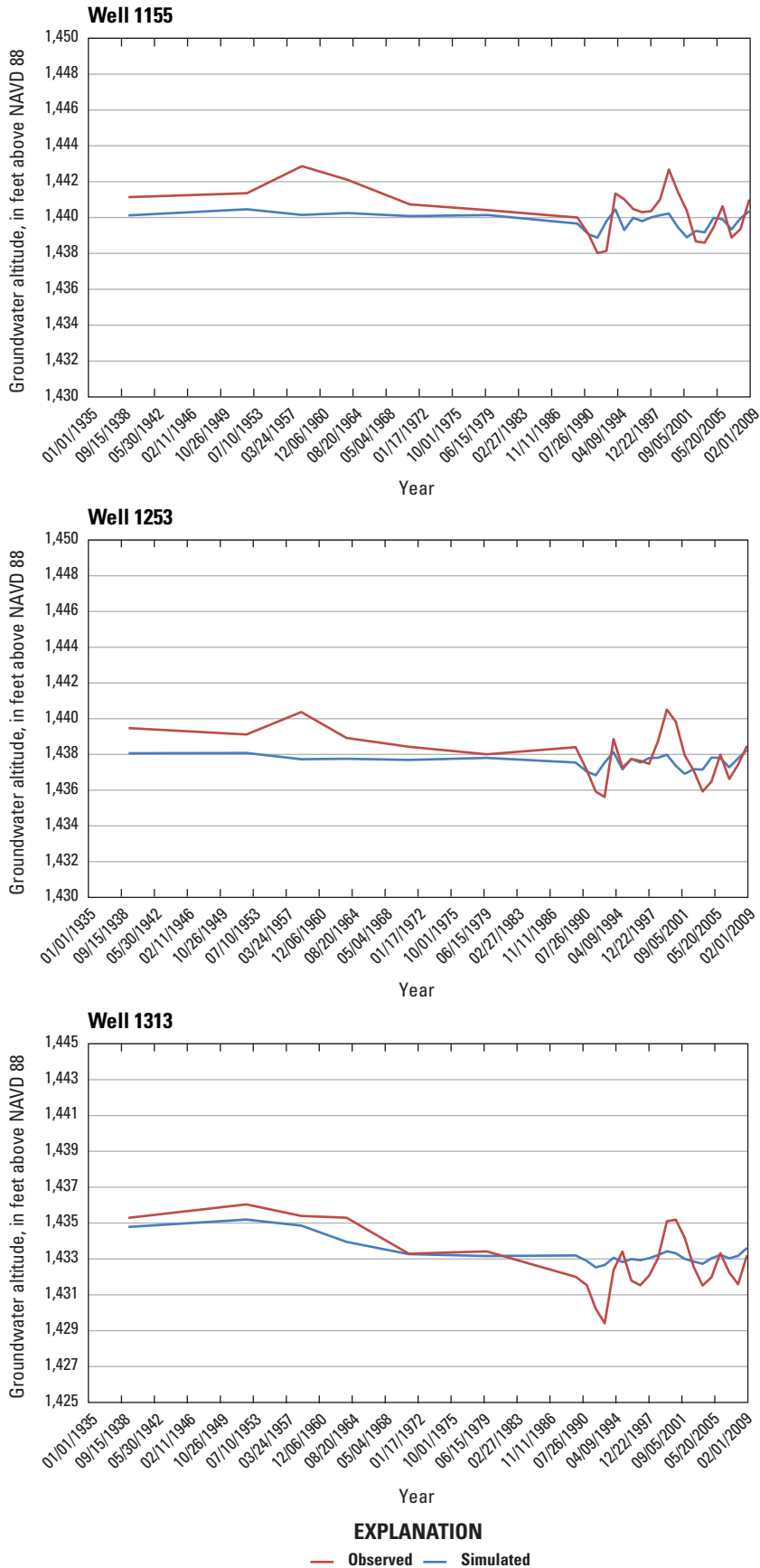


Figure 40. Simulated and observed groundwater levels for selected wells.—
Continued

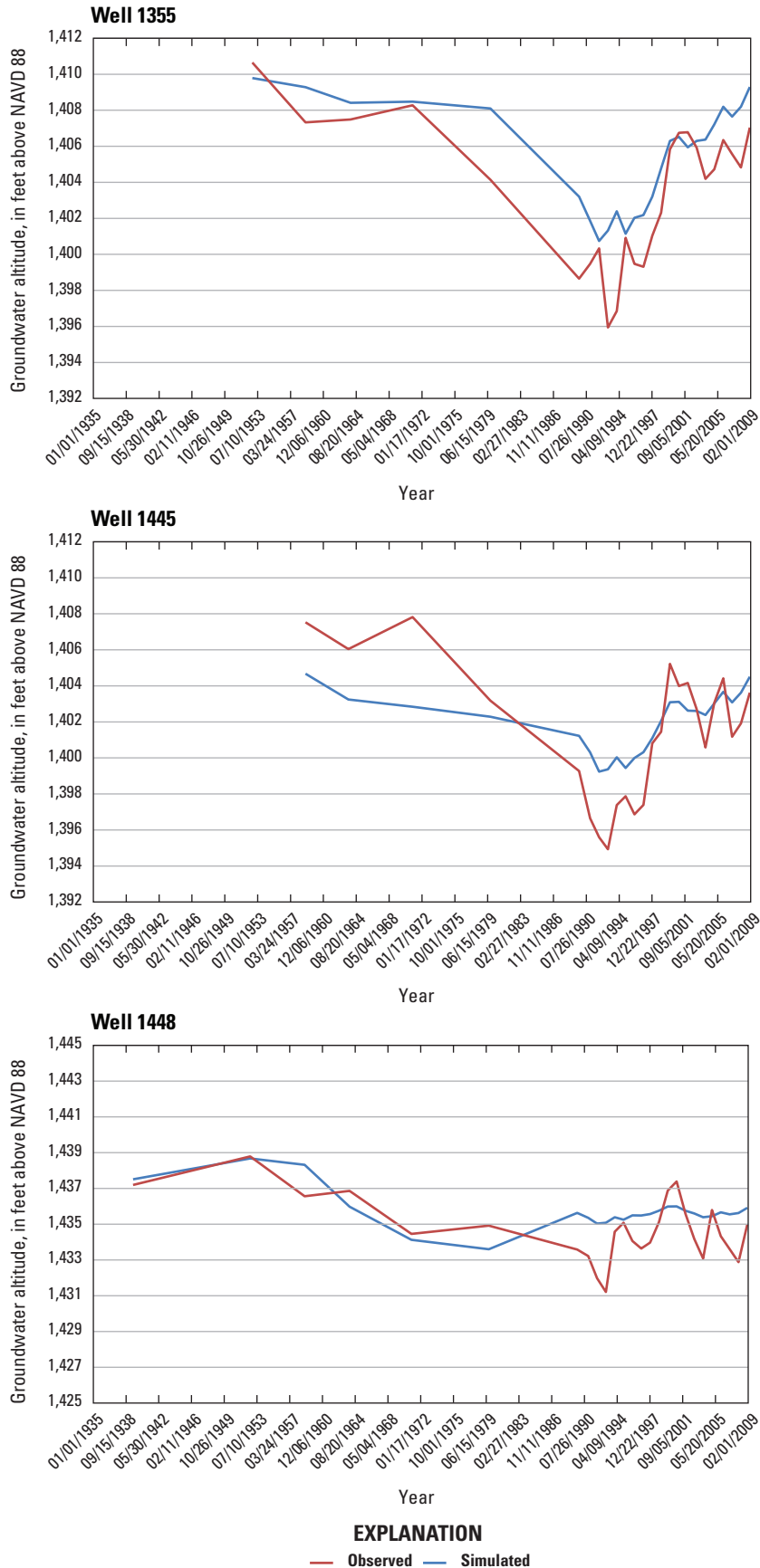


Figure 40. Simulated and observed groundwater levels for selected wells.—
Continued

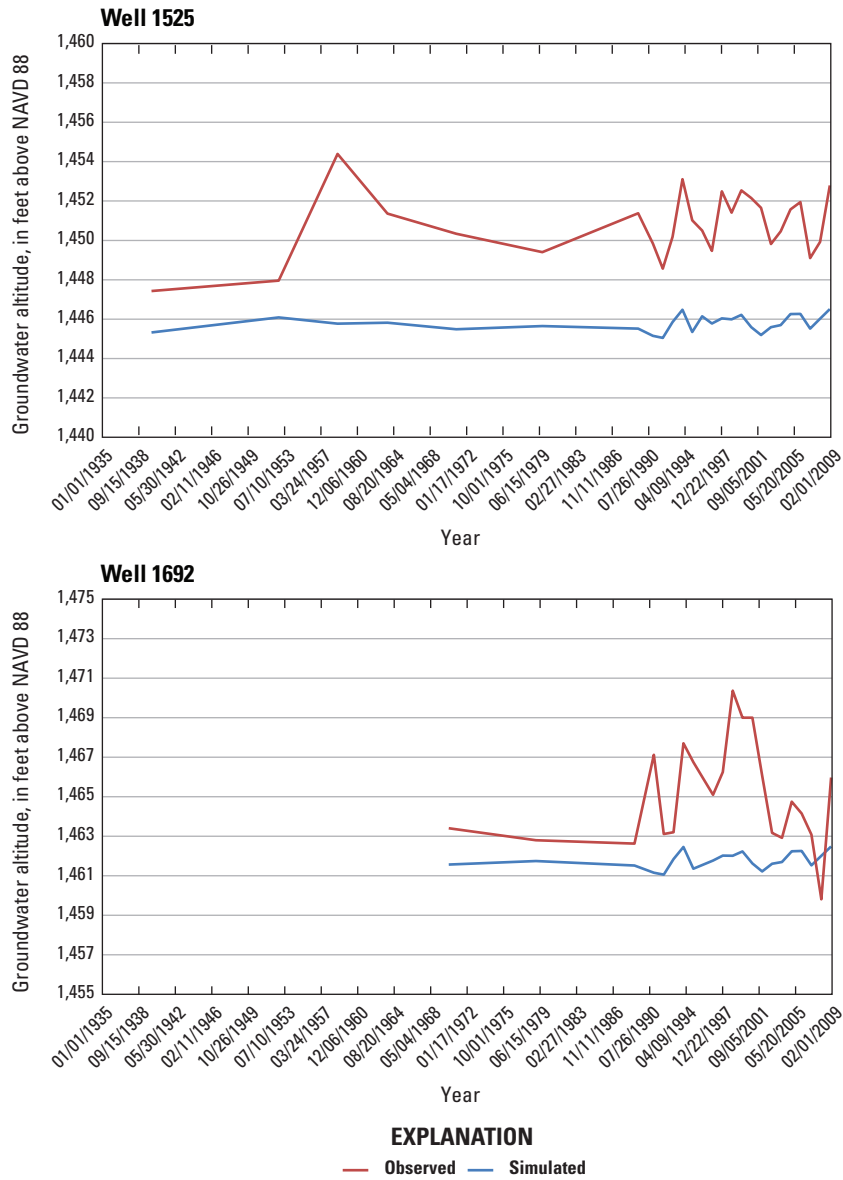


Figure 40. Simulated and observed groundwater levels for selected wells.—
Continued

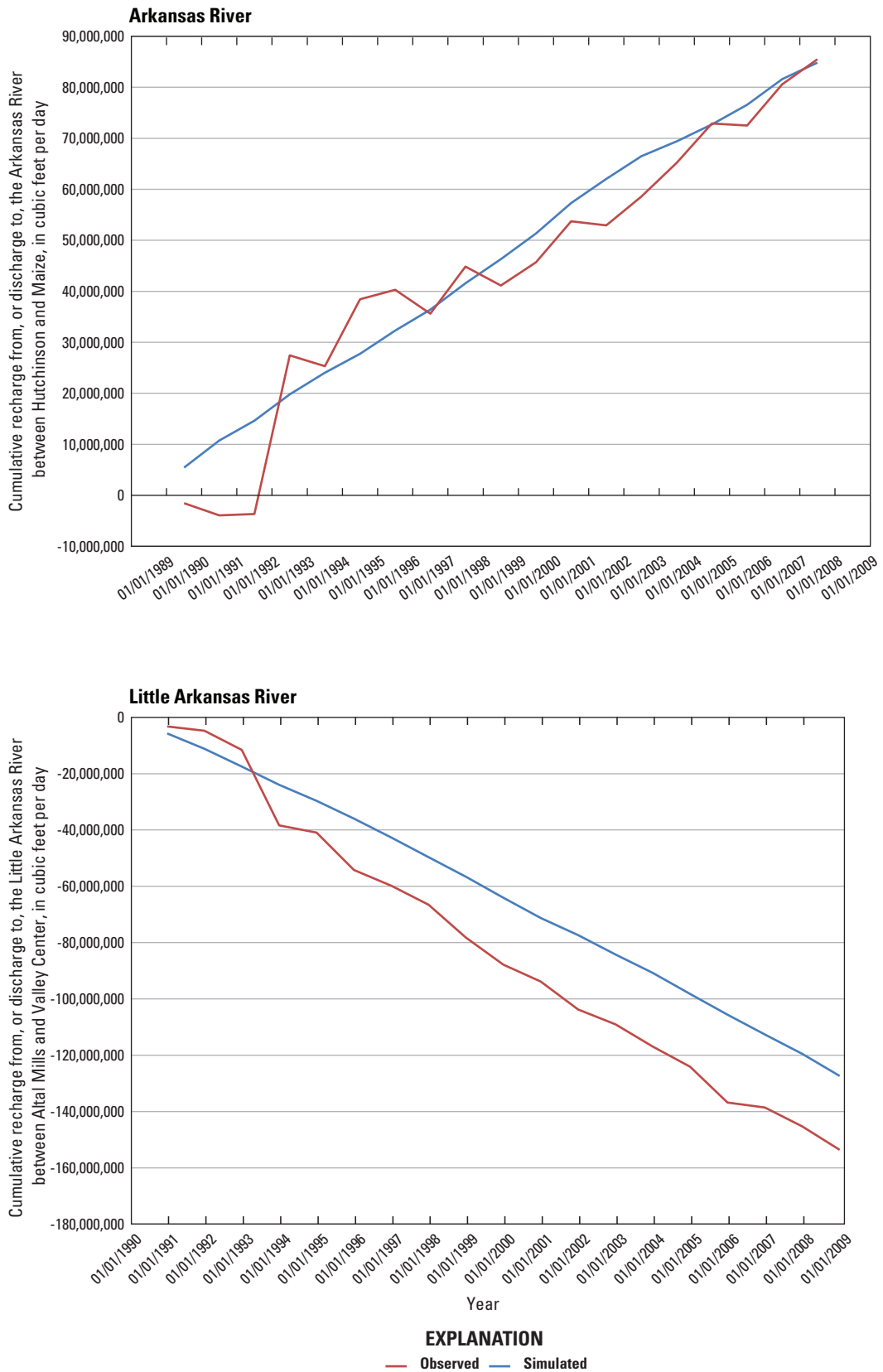


Figure 41. Observed and simulated cumulative streamflow gains and losses for the Arkansas and Little Arkansas Rivers for the transient simulation.

considered insensitive to that parameter. In addition, calculated sensitivities depend on the existence of observation data. If observations are not available in an area of the model, changes to a parameter may cause large changes to hydraulic head or flows, but the sensitivity of those parameters will not reflect the large effect they may have.

Composite scaled sensitivities were calculated by MODFLOW-2000 using dimensionless scaled sensitivities for all observations. The relative values of composite scaled sensitivities are used to indicate the total amount of information provided by the observations for the estimation of a parameter (Hill, 1998). Composite scaled sensitivities for selected parameters are shown for the steady-state and transient calibration simulations in figure 42. The model is more sensitive to a parameter with a large composite sensitivity value than to a parameter with a small value.

Composite sensitivities are smaller for the steady-state calibration simulation compared to the transient calibration simulation because there are fewer observations available in the steady-state simulation. In both simulations, parameters with larger composite sensitivities have a large areal distribution. For the steady-state simulation, the 10 parameters with the largest composite sensitivities are RECH2, L1-Z4, L1-Z3, RECH1, RECH6, RECH4, RECH5, L2-Z4, L1-Z2, and VK1. Recharge (fig. 27) and vertical conductance in model layer 1 (fig. 24) affect heads in all areas of the model. The hydraulic conductivity parameter zones L1-Z4, L1-Z3, and L1-Z2 (fig. 21) are present in the area of the Wichita well field and basin storage area. Hydraulic conductivity zone L2-Z4 (fig. 22) also is widely distributed. For the transient calibration simulation, the 10 parameters with the largest composite sensitivities are EVAP, RECH6, RECH5, L1-Z7, RECH4, L2-Z5, L1-Z6, L1-Z5, L1-Z4, and L3-Z5. For the transient calibration simulation, evapotranspiration and recharge affect heads in all areas of the model, and, as was indicated for the steady-state calibration simulation, hydraulic conductivity zones with a large distribution also have large composite sensitivities. The larger composite sensitivities for hydraulic conductivity parameters L2-Z5 and L3-Z5 are most likely because they are located near the Arkansas and Little Arkansas rivers and their value affects flow between the rivers and the aquifer.

One-percent scaled sensitivities are calculated by MODFLOW-2000 and approximately equal the amount that the simulated values would change if the parameter values increased by one percent (Hill, 1998). For observations related to flows between the aquifer and streams, positive sensitivities indicated an increase in flow from the river to the aquifer (or decrease in flow from the aquifer to the river); negative sensitivities indicated an increase in flow from the aquifer to the river or decrease in flow from the river to the aquifer. For groundwater-level observations, positive sensitivities indicate an increase in head with an increase in parameter value; negative sensitivities indicate a decrease in head with an increase in parameter value. Different 1-percent sensitivities for groundwater-level observations are caused by the proximity of the well to the area of the model that the

parameter affects and its value. One-percent scaled sensitivities from the transient calibration simulation are shown in figure 43 for selected parameters and groundwater-level observations (observed and simulated hydrographs shown in fig. 40) and stream observations (observed and simulated hydrographs shown in fig. 41).

Scaled 1-percent sensitivities were positive for recharge for all groundwater observations and increasing recharge resulted in increased simulated groundwater levels. Scaled 1-percent sensitivities were positive and negative for hydraulic conductivity for groundwater-level observations, indicating the response of groundwater levels to changes in hydraulic conductivity is complex. Increasing hydraulic conductivity typically lowers groundwater levels and decreasing hydraulic conductivity raises groundwater levels; however, the opposite effect can occur when flow into and flow out of the aquifer is affected by aquifer hydraulic conductivity. For example, for well 733, increasing hydraulic conductivity in model layer 1 for L1-Z4, L1-Z5, and L1-Z6 causes simulated groundwater levels to increase, but increasing hydraulic conductivity for L1-Z1, L2-Z2, or L3-Z3 causes simulated groundwater levels to decrease. Increasing hydraulic conductivity in model layer 1 most likely increases the amount of recharge to model layer 2 where well 733 is screened, whereas increasing hydraulic conductivity in model layers 2 and 3 allows groundwater to flow more quickly in these model layers, thus lowering groundwater levels. Simulated groundwater levels increase near wells 1037 and 1038 when L1-Z4 is increased but decrease when L1-Z5 is increased. For these well locations, L1-Z4 defines the hydraulic conductivity in the area and there are numerous pumping wells. Increasing the hydraulic conductivity increases groundwater flow to the pumping wells and reduces drawdown in the area. Hydraulic conductivity parameter L1-Z5 is located adjacent to the Little Arkansas River. Increasing the value for L1-Z5 increases groundwater discharge to the Little Arkansas River and lowers groundwater levels in the area. For wells 1525 and 1692 that are located in the dune sand area, increasing recharge raises groundwater levels and increasing evapotranspiration lowers groundwater levels. In this area, low values of hydraulic conductivity (fig. 21) limit the downward movement of groundwater, and recharge and evapotranspiration have the most effect on groundwater levels.

Flow between the Arkansas River and the *Equus* Beds aquifer is affected most by changes in recharge (fig. 27) and hydraulic conductivity (figs. 21, 22, and 23). Increasing recharge either increases flow from the aquifer to the Arkansas and Little Arkansas Rivers or decreases flow from the rivers to the aquifer. Increasing evapotranspiration has a large effect on the Arkansas River but a small effect on the Little Arkansas River. This is most likely the result of larger rates of evapotranspiration near the Arkansas River because of shallow depth to groundwater. Evapotranspiration is less near the Little Arkansas River because well pumping has increased depth to groundwater. Increasing hydraulic conductivity in areas near the rivers increases the rate of water flow between the rivers

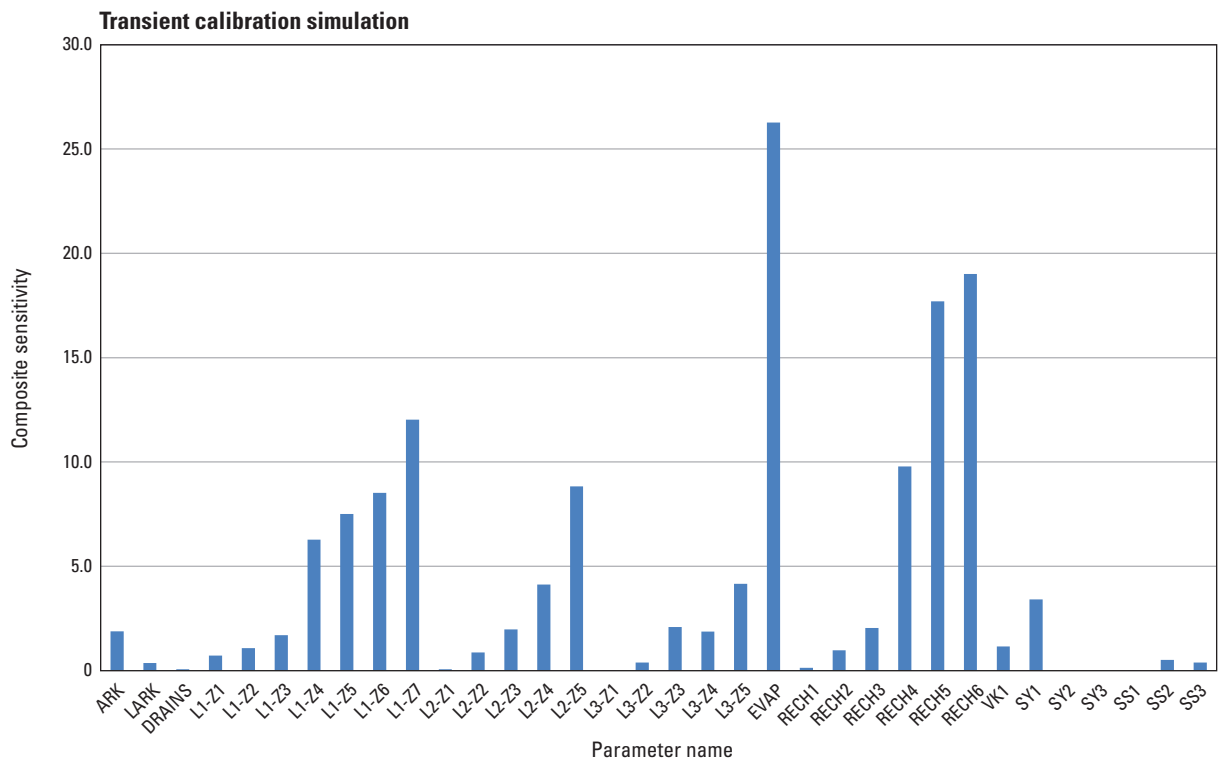
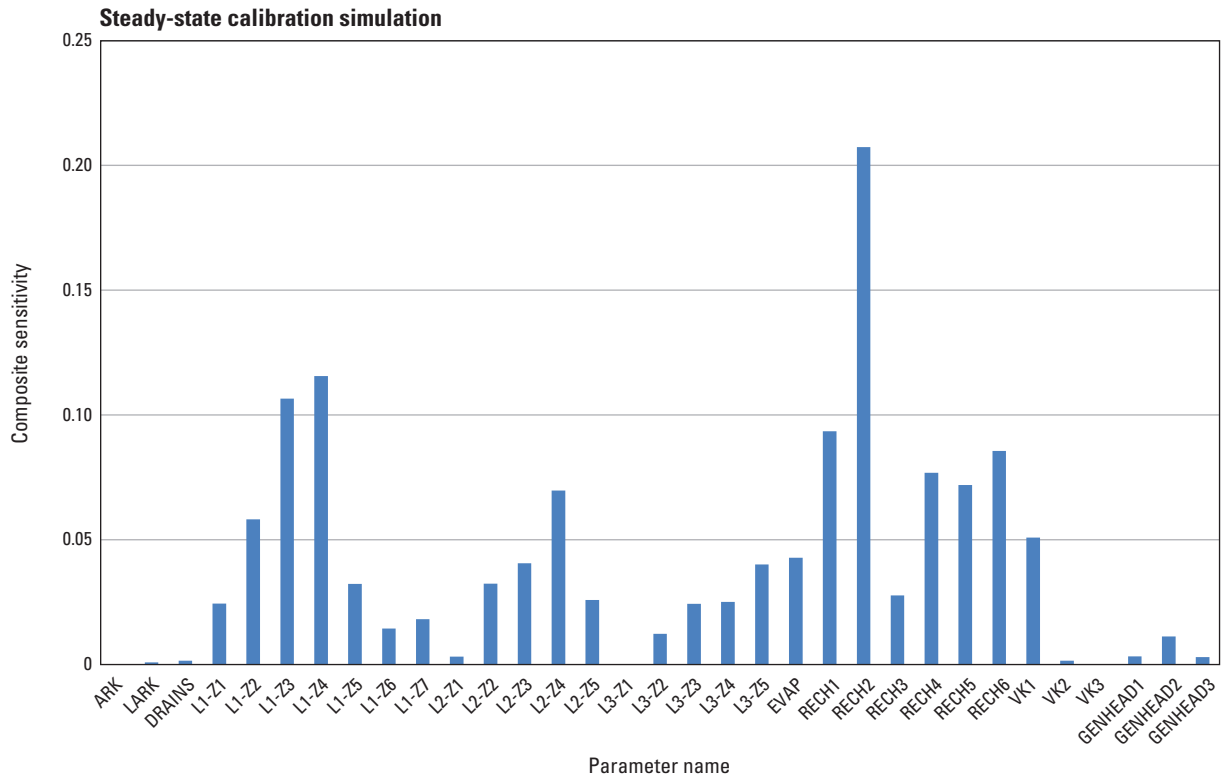


Figure 42. Composite scaled sensitivities for model input parameters from the steady-state and transient calibration simulations.

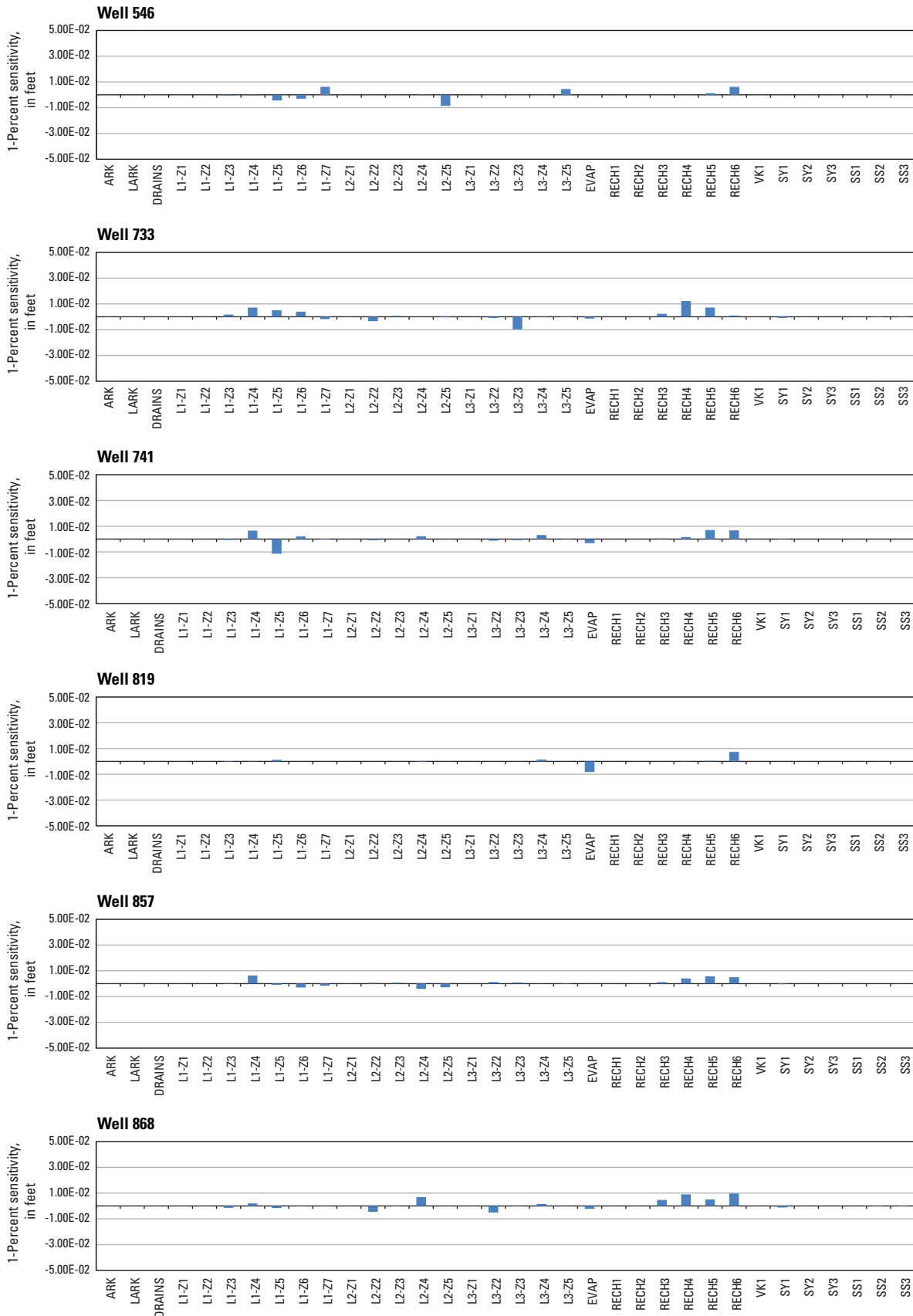


Figure 43. One-percent scaled sensitivities of parameters for selected stream and groundwater-level observations for the transient calibration simulation.

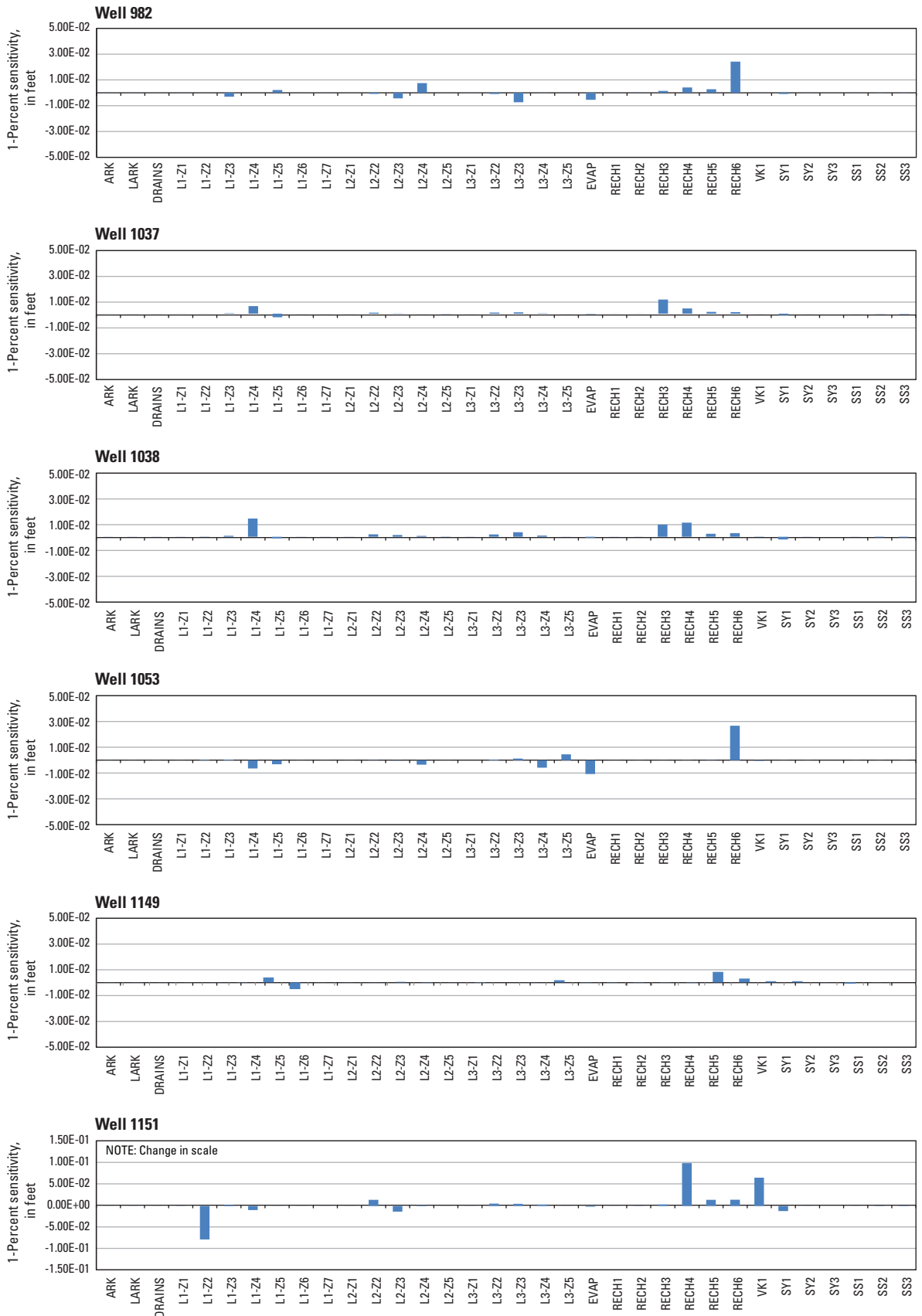


Figure 43. One-percent scaled sensitivities of parameters for selected stream and groundwater-level observations for the transient calibration simulation.—Continued

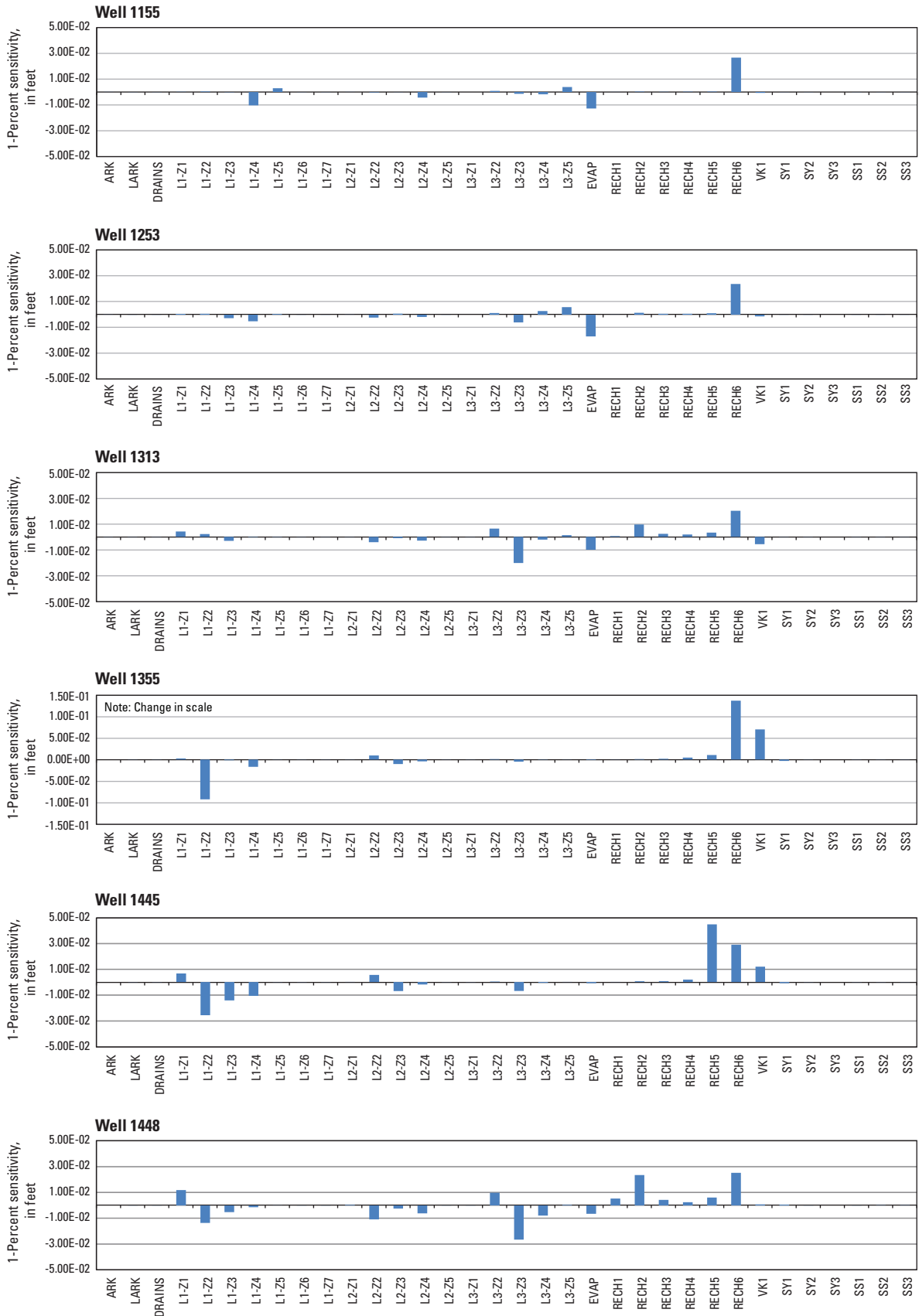


Figure 43. One-percent scaled sensitivities of parameters for selected stream and groundwater-level observations for the transient calibration simulation.—Continued

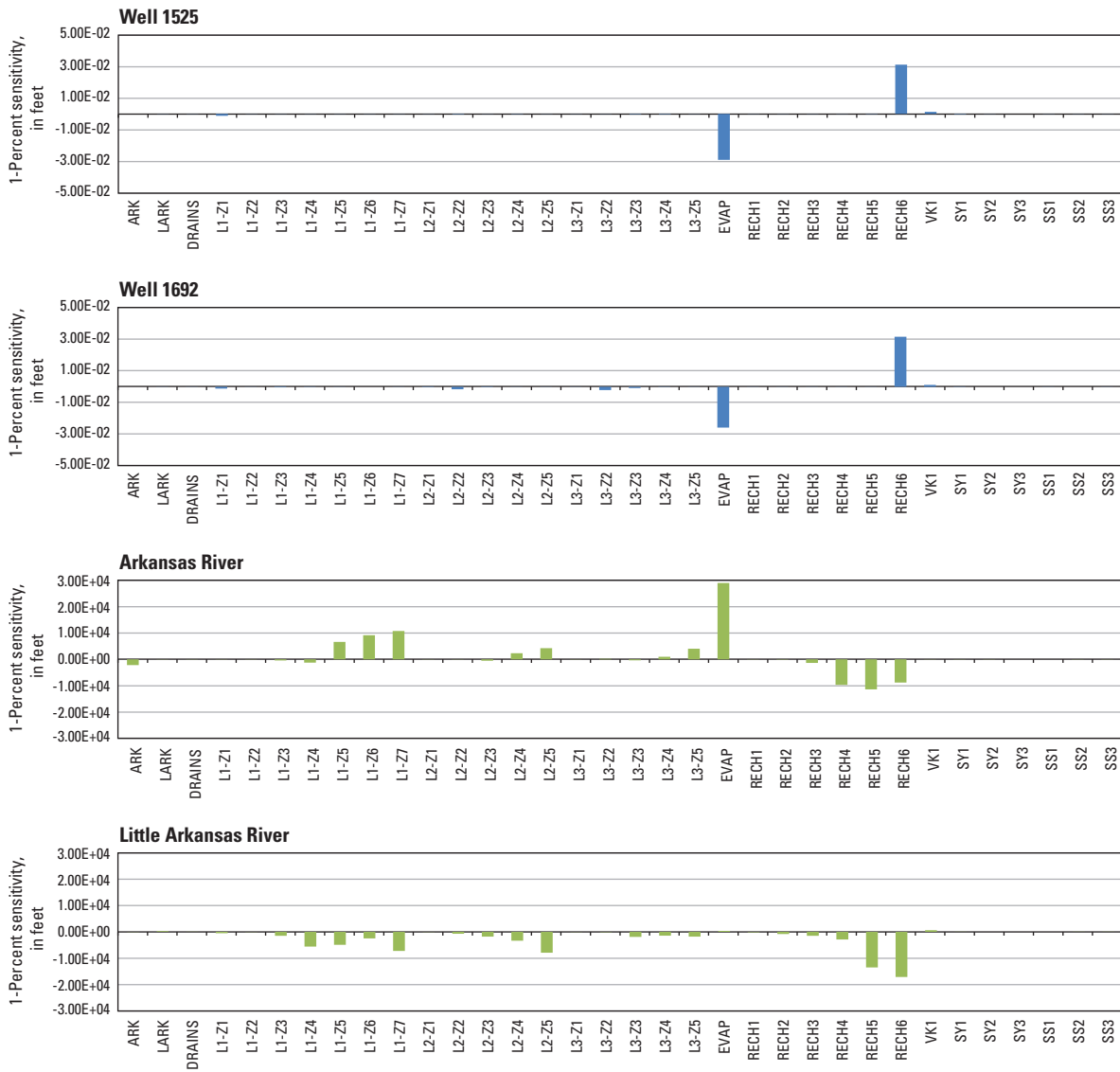


Figure 43. One-percent scaled sensitivities of parameters for selected stream and groundwater-level observations for the transient calibration simulation.—Continued

and the aquifer. For the Arkansas River, flow from the river to the aquifer increased with increasing hydraulic conductivity but for the Little Arkansas River, flow from the aquifer to the river is increased.

Model Limitations

A groundwater model is a simplification of actual conditions. The accuracy of the groundwater model results depend on the accuracy of the input data and the accuracy of the equations used to characterize groundwater flow. The groundwater-flow model for this study was constructed with available hydrologic data to simulate groundwater flow in the *Equus* Beds aquifer in the study area. To correctly interpret model results, the following limitations of the model should be considered.

1. Model parameters such as hydraulic conductivity and recharge are applied uniformly to groups of model cells or zones. The assumption of uniformity likely is inaccurate because geologic materials and factors affecting groundwater flow are typically nonuniform.
2. The groundwater-flow model was discretized using a grid with cells measuring 400 ft by 400 ft. Model results were evaluated on a relatively large scale and cannot be used for detailed analyses such as simulating water-level drawdown near a single well. A grid with smaller cells would be needed for such detailed analysis.
3. The time discretization is too coarse to capture episodic floods or heavy precipitation events.
4. Recharge rates, evapotranspiration rates, specific yield, storage coefficient, and streambed conductance values are artifacts of model calibration. Field measurements of these parameters would provide more reliable values as model input.
5. The unsaturated zone, a part of the groundwater flow system overlying the aquifer, is not simulated.
6. Average annual rates for production well pumping were used in the groundwater-flow model. Average pumping rates may introduce error if water-level observations from monitoring wells located close to pumping wells are obtained when the wells are pumping at a rate that is different than the average used in the model. In this case, matching the simulated water levels to observed water levels during calibration may either overestimate or underestimate hydraulic properties of the aquifer near the monitoring well.

Artificial-Recharge Accounting

The ability of the calibrated model to account for the additional water recharged to the *Equus* Beds aquifer as part of the ASR project was assessed using the USGS subregional water budget program ZONEBUDGET (Harbaugh, 1990), and by comparing those results to metered recharge for 2007 and 2008 and previous estimates of artificial recharge (Burns and McDonnell, 2008, 2009). A programming error in

MODFLOW-2000 with respect to ZONEBUDGET calculations was corrected in MODFLOW-2005 (Harbaugh, 2005), which was used for artificial-recharge accounting simulations in this report. Model input is identical although there are small differences in components of the flow budget output between the two programs. ZONEBUDGET used the cell by cell flow data from MODFLOW to calculate water-flow budgets for each index cell (fig. 3) of the BSA within the groundwater model. Phase I of the ASR project was completed in 2006 and large-scale artificial recharge of the aquifer began at the phase I sites in March 2007. Groundwater flow was simulated from 1935 through 2008 and groundwater flow budgets were calculated for 2007 and 2008 for each index cell in the BSA. Initial conditions for the accounting simulations were obtained from the steady-state calibration simulation. For 1935 through 2006, the stress periods and stresses from the transient calibration simulation were used as model input. For 2007 and 2008, stress periods and stresses from the transient calibration simulation were used as model input for the artificial-recharge (AR) simulation and stress periods, and stresses from the transient calibration simulation, except for artificial-recharge well pumping, were used as model input for the no artificial-recharge (NAR) simulation. To calculate the effects of artificial recharge on groundwater flow in the BSA, results from the NAR simulation were subtracted from results from the AR simulation. With identical model input, except for artificial-recharge operation, the difference in simulated flows estimates the change in flows caused by artificial recharge. For transient groundwater flow, the rate of outflow equals the rate of inflow plus the rate that water is released from storage. The change in storage between the AR and NAR simulations is the volume of water that estimates the recharge credit for the aquifer storage and recovery system. Simulated groundwater flow budgets of the total modeled area for the AR and NAR simulations for 2006 through 2008 are listed in table 13. The amount of artificial recharge applied to each recharge basin and well in 2007 and 2008 and the BSA index cell where the basin or well is located is listed in table 14.

The change in storage between AR and NAR simulations for 2007 was 1,107 acre-ft and metered recharge was 963 acre-ft for the total model area. For 2008 the simulated change in storage was 684 acre-ft and metered recharge was 833 acre-ft. Total simulated change in storage was 1,790 acre-ft and total metered recharge was 1,796 acre-ft. Increased well pumping (inflow from artificial recharge and outflow from well pumping) is the largest difference between the AR and NAR simulations for 2007 and 2008 followed by changes in storage and river flows. Although pumping was larger in the AR simulation because of diversion wells located next to the Little Arkansas River near Halstead, Kans., the increased pumping was offset largely by increased flow into the model from the Little Arkansas River and decreased flow to the Little Arkansas River as groundwater that would have discharged to the river was intercepted by the pumping wells. The increased storage resulting from artificial recharge in the model was in the BSA where phase 1 artificial-recharge sites are located.

The drought during the 1950s and groundwater pumpage from the aquifer near the Wichita well field for production and agricultural use between 1940 and 1957 caused a substantial water level decline in and near the Wichita well field (Hansen and Aucott, 2004). Increased irrigation pumpage during the 1970s and 1980s caused further declines in groundwater levels (Myers and others, 1996; Aucott and Myers, 1998). Most of the water-level declines were caused by groundwater pumpage but the effects of climate on recharge also have affected water levels (Hansen and Aucott, 2003). Groundwater level altitudes in parts of the aquifer near the Wichita well field (fig. 1) increased by more than 20 ft between 1992 and 2006. Other factors contributing to water-level increases include subsurface inflow, streamflow losses, and irrigation return flow (Myers and others, 1996).

In areas where the aquifer is well connected hydraulically, shallow and deep groundwater levels are similar; however, in areas where the aquifer is semi-confined, substantial differences in shallow and deep groundwater levels exist (Hansen and Aucott, 2003). The dune sands in the northwest part of the study area (fig. 4) contain layers of silt and clay that limit the downward movement of water (Myers and others, 1996), as indicated by the existence of interdune ponds (Williams and Lohman, 1949) and shallow water levels in closely spaced wells that are 27 ft higher than deeper water levels (Williams and Lohman, 1949). Although downward movement of groundwater is limited in this area, the existence of a groundwater mound in the *Equus* beds deposits below the sand dune area indicates recharge through the sand dunes is larger than in surrounding areas (Myers and others, 1996).

Groundwater-Flow Directions

Groundwater flow within the aquifer in the area between the Arkansas and Little Arkansas Rivers generally is west to east and groundwater flow in the area north of the Little Arkansas River is from north to south. Groundwater level maps from 1940 and 1989 (Myers and others, 1996) illustrate the general flow of groundwater in the *Equus* Bed aquifer at these times (figs. 10 and 11). Groundwater withdrawals create localized cones of depression around each well or well field that may alter regional groundwater to flow toward the wells. A cone of depression generally has the shape of an inverted cone with the lowest part centered at the pumping well. Although cones of depression around wells are not visible at the scale shown in figures 10 and 11, increased well pumping in 1989 along and west of the Little Arkansas River has lowered the water table and altered groundwater flow directions compared to 1940 conditions.

Groundwater/Surface-Water Interaction

Long-term withdrawal of groundwater from the *Equus* Beds aquifer lowered groundwater-levels in the area of the

Wichita well field (Hansen and Aucott, 2003). Seepage runs conducted in the 1980s and 1990 indicate that the Arkansas River in the study area either gained or lost water in the upper reach (upstream from the point midway between the streamflow gages near Maize (07143375) and Hutchinson (07143330), fig. 6) but lost water in the lower reach that is adjacent to the area of lowered groundwater levels (Myers and others, 1996).

Streamflow, estimated base flow (Lim and others, 2005; Sloto and Crouse, 1996), and the difference in base flow are shown for the Arkansas River for the streamflow gages near Hutchinson (07143330) and Maize (07143375) from December 1989 through 2008 in figure 12 and for the Little Arkansas River for the streamflow gages at Alta Mills and Valley Center from December 1989 through 2008 in figure 13. As shown in figure 12, the Arkansas River is a gaining stream between the streamflow gages at Hutchinson (07143330) and Maize (07143375) during high flows most likely associated with times of increased recharge to the *Equus* Beds aquifer; however, during low flow most likely associated with decreased recharge, the Arkansas River is a losing stream in this reach. As shown in figure 13, the Little Arkansas River is a gaining stream between the streamflow gages at Alta Mills and Valley Center from 1989 through 2008 with base flow increasing during high flows most likely associated with times of increased recharge to the *Equus* Beds aquifer and decreasing during low flows most likely associated with periods of decreased recharge.

Methods

This section describes the methods used to simulate groundwater flow and includes discussion of the computer software and the equation used to simulate groundwater flow. Spatial and temporal discretization of the finite-difference groundwater-flow model is discussed and the hydrogeologic framework is described. Parameter values, associated model zones, and the hydraulic properties of the *Equus* Beds aquifer are listed and illustrated. Boundary conditions required to simulated groundwater flow are discussed including recharge, evapotranspiration, streamflow, well pumping, and lateral boundaries of the aquifer where groundwater flows into, or out of, the model area. Observations of head and streamflow are described. The techniques used and criteria for model calibration are discussed including initial conditions, steady-state calibration, transient calibration, and parameter sensitivity. A comparison between simulated and measured groundwater level change for selected times is presented and the limitations of the model are listed and discussed.

Groundwater Flow Simulation

Groundwater flow was simulated for the *Equus* Beds aquifer using the three-dimensional finite-difference

groundwater-flow model MODFLOW-2000 (Harbaugh and others, 2000). MODFLOW-2000 is a modified version of MODFLOW (McDonald and Harbaugh, 1988) that incorporates the use of parameters to define model input and the calculation of parameter sensitivities. In addition, the code incorporates the modification of parameter values to match observed heads, flows, or advective transport using the observation, sensitivity, and parameter-estimation processes described by Hill and others (2000).

Three-dimensional simulation of groundwater flow in the *Equus* Beds aquifer was necessary to accurately determine the hydraulic-head distribution in the aquifer. Substantial differences in shallow and deep groundwater levels exist (Hansen and Aucott, 2003) in areas where the aquifer is semi-confined. Discharge from the aquifer to rivers may vary according to river size, depth of the streambed, or streambed conductance. Groundwater flow may be divided into smaller flow subsystems because of the degree of interaction between groundwater, the well fields, and the larger and smaller rivers in the study area. Pumping from the well fields located near a river can induce flow from the river and cause groundwater flow beneath the river.

The following equation was the governing equation used in MODFLOW-2000 to approximate groundwater flow rates in three dimensions:

$$\frac{\partial}{\partial x} \left(K_x \frac{\partial h}{\partial x} \right) + \frac{\partial}{\partial y} \left(K_y \frac{\partial h}{\partial y} \right) + \frac{\partial}{\partial z} \left(K_z \frac{\partial h}{\partial z} \right) - W = S_s \frac{\partial h}{\partial t} \quad (1)$$

where

- $K_x, K_y,$ and K_z are the values of hydraulic conductivity along the $x, y,$ and z coordinate axes and are assumed to be parallel to the major axes of hydraulic conductivity, in feet per day;
- h is the potentiometric head, in feet;
- W is a volumetric flux per unit volume and represents sources or sinks, or both, of water, such as well discharge, leakage through confining units, streambed leakage, recharge, and water removed from the aquifer by drains, per day;
- S_s is the specific storage of the porous material, per foot; and
- t is time, in days.

Initial Conditions

Initial conditions for the transient calibration simulation were obtained from the steady-state calibration simulation. These initial conditions included the head distribution simulated using average hydrologic conditions from 1935 through 1939 and recharge, evapotranspiration, streamflow, general head boundary conditions, and well pumping.

Spatial and Temporal Discretization

The modeled area covers almost 1,845 square miles including the entire study area shown in figure 1. The model has uniform cells 400 ft per side and contains 963,900 cells in 510 rows, 630 columns, and 3 model layers. Model layer 1 is the topmost, model layer 2 is the middle layer, and model layer 3 is the bottom layer. Model layer thickness and areal extent are shown for model layer 1 in figure 14, model layer 2 in figure 15, and model layer 3 in figure 16. The regular grid spacing facilitated data input from a Geographic Information System (GIS) and analysis of model output by the GIS. The small size of each cell limits the error associated with particle tracking and solute transport, which are potential uses for the model. Cells containing sinks that do not discharge at a rate large enough to consume all the water entering the cell introduce uncertainty into the computed path of the imaginary particle. The irregular shape of the active model boundary reduced the number of active cells in the model to 369,346 with 177,572 active cells in model layer 1 (fig. 14); 123,265 active cells in model layer 2 (fig. 15); and 68,509 active cells in model layer 3 (fig. 16).

The model simulates steady-state and transient conditions. Steady-state conditions were simulated using average hydrologic conditions from 1935 through 1939 that include recharge, evapotranspiration, streamflow, flow across model boundaries, and well pumping. Transient conditions including recharge, evapotranspiration, streamflow, flow across model boundaries, and well pumping were simulated from 1935 to 2008 using 26 stress periods. Stress periods 1 through 7 simulate groundwater flow from 1935 through 1989 and stress period lengths are from Myers and others (1996). Yearly stress periods 8 through 26 simulate groundwater flow from 1990 through 2008 and allow simulation of changes in areally distributed recharge based on average annual precipitation. Stress periods, time steps, and time-step multipliers are listed in table 1 for all stress periods.

Table 1. Transient groundwater simulation stress periods, stress period start date, stress period length, time steps, and time-step multipliers.

Stress period	Stress period start date	Stress period length	Time steps	Time-step multiplier ¹
1	January 1, 1935	5 years	50	1.01
2	January 1, 1940	13 years	50	1.01
3	January 1, 1953	6 years	50	1.01
4	January 1, 1959	5 years	50	1.01
5	January 1, 1964	7 years	50	1.01
6	January 1, 1971	9 years	50	1.01
7	January 1, 1980	10 years	50	1.01
8 to 26	January 1, 1990	1 year	50	1.01

¹The time-step multiplier is used by MODFLOW to calculate a geometric increase in the length of each time step within a stress period.

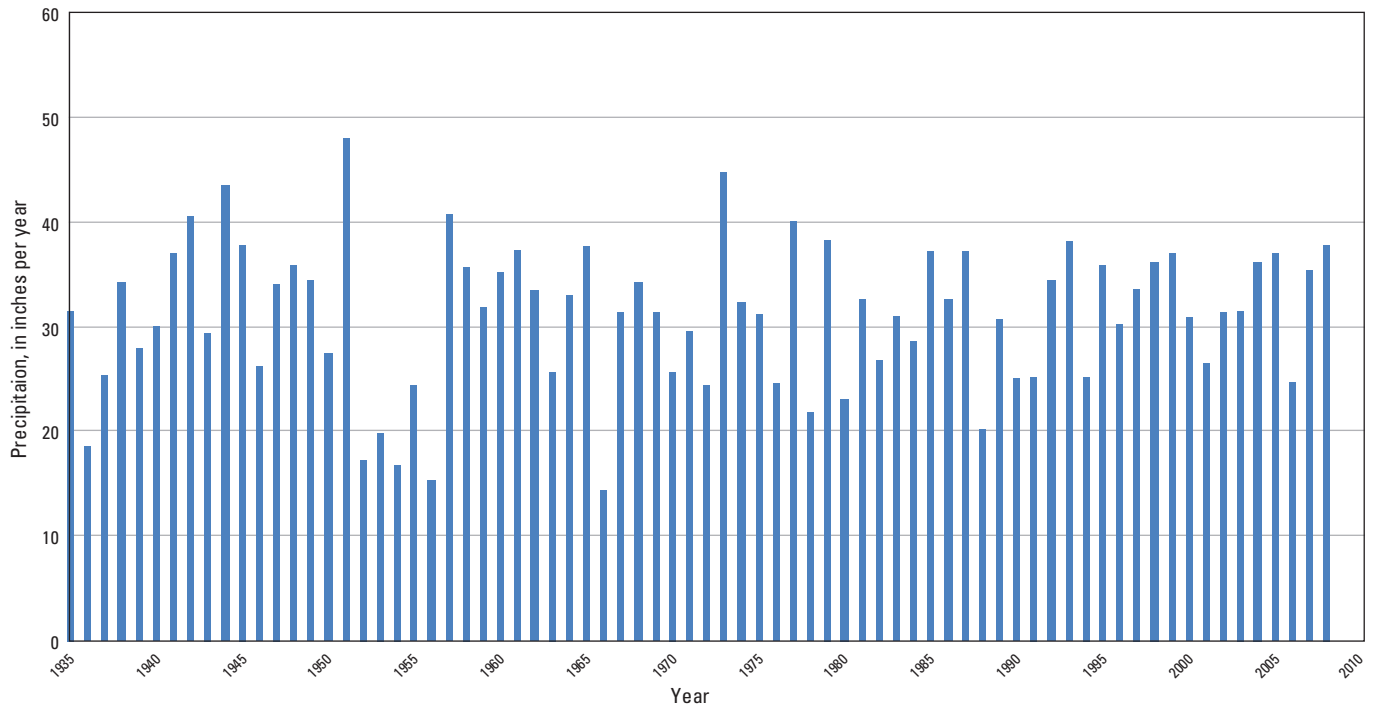


Figure 25. Average annual precipitation in inches per year for weather stations at Hutchinson (143930), Mt. Hope (145539), Newton (145744), Sedgwick and Halstead (143366) and Wichita (148830) near the Wichita well field (National Oceanic and Atmospheric Administration, 2008).

The average number of daylight hours per day was calculated for a point near the center of the model area, at Halstead, Kans. (longitude 97°31'00" W, latitude 38°00'00" N). Sunrise and sunset times were obtained from the Astronomical Applications Department, U.S. Naval Observatory (http://aa.usno.navy.mil/data/docs/RS_OneYear.php). Temperature data from Newton, Kans. were used for the computation because a complete record was available from National Climate Data Center Archives (<http://lwf.ncdc.noaa.gov/oa/climate/stationlocator.html>). Initial estimated evapotranspiration was altered during calibration to more closely match observed and simulated groundwater levels.

Streams

The Arkansas River, Little Arkansas River, and their tributaries are represented in the model as head-dependent flux boundaries. The Arkansas River, Little Arkansas River, and Cow Creek (near Hutchinson, Kans.) were simulated in MODFLOW-2000 using the River Package and the smaller streams and tributaries were simulated using the Drain Package (McDonald and Harbaugh, 1988). All rivers and drains are within model layer 1.

Flow into or out of the aquifer at each of the cells where a river is simulated is a function of the river stage with respect to the altitude of the potentiometric surface, the hydraulic conductivity of the streambed material, the cross-sectional area of flow between the stream and the aquifer, and the altitude of the water table with respect to the altitude of the

streambed (McDonald and Harbaugh, 1988). Stream stages in the Arkansas and Little Arkansas Rivers were recorded at streamflow gages (fig. 6) hourly (U.S. Geological Survey, 2009a) and average annual stage was calculated for each gage. The average annual altitude of the river surface used in each stress period of each simulation was assigned to each model cell with a stream by interpolating the specified river surface altitude between gaging stations. Each stream was assigned a single value for streambed hydraulic conductivity. The area of the stream within each model cell was calculated and the streambed hydraulic conductivity value was multiplied by the area of the stream and then divided by the thickness of the streambed to determine the streambed conductance. Streambed thicknesses are unknown and were assigned an arbitrary value of 1 ft. Initial streambed conductances were altered during calibration to more closely match observed and simulated flow between the streams and the aquifer.

Flow into or out of the aquifer at each of the cells where a drain is simulated is a function of the altitude of the potentiometric surface, the hydraulic conductivity of the drain bed material, the cross-sectional area of flow between the drain and the aquifer, and the altitude of the water table with respect to the altitude of the drain bed (McDonald and Harbaugh, 1988). Each stream simulated as a drain was assigned a single value for streambed hydraulic conductivity. The area of the stream within each model cell was calculated and the initial streambed hydraulic conductivity value was multiplied by the area of the stream and then divided by the thickness of the streambed to determine the streambed conductance.

Streambed thicknesses are unknown and were assigned an arbitrary value of 1 ft. Initial streambed conductances for drains were altered during calibration to more closely match observed and simulated flow from the aquifer to the drains. Simulated rivers and drains are shown in figure 28.

Wells

Pumping wells are internal boundaries of the model where water was removed at a specified rate equal to the discharge of each well. The total volume of water withdrawn annually from the aquifer by pumping from irrigation, production, and industrial wells was obtained from each water supplier when available or from the KDA-DWR Water Rights Information System database (Kansas Department of Agriculture—Division of Water Resources, unpub. data, 2009). The depth of each pumping well was based on the screened interval, when known, or the depth of the well. The Multinode Well Package was used to simulate all industrial, irrigation and production well pumping (Harbaugh and others, 2000). The MultiNode Well Package vertically distributes pumping between model layers from each well based on the top and bottom altitudes of the screened interval and the hydraulic properties of each model layer.

Groundwater pumpage data for 1935 to 1979 were obtained from Spinazola and others (1985) and Myers and others (1996). Groundwater pumpage for the stress periods from 1935 through 1979 was distributed in the model based on the spatial and temporal distribution of pumping in Spinazola and others (1985). The model cells from Spinazola and others (1985) are 1 mile on each side and pumping was assigned to the center of each cell. Pumping wells were placed in the current model to coincide with the center of each cell in the model from Spinazola and others (1985). Pumping was distributed vertically across all model layers by using the MultiNode Well Package. Locations of simulated pumping wells for 1935 through 1979 are shown in figure 29.

Annual groundwater pumpage data for industrial, irrigation, and production wells in the study area for 1988 through 2008 were obtained from the KDA-DWR (Kelly Emmons, Kansas Department of Agriculture, Division of Water Resources, written commun., June 5, 2009, and August 31, 2009). Groundwater pumpage for the stress period from 1980 through 1989 was distributed in the model using well locations and pumping rates from 1989. Groundwater pumpage for the stress periods from 1990 through 2008 was distributed in the model using well locations and average annual pumping rates.

Monthly pumpage data for Wichita's production wells for 1990 through 1993 and 1995 through 2008 (Megan Schmeltz, city of Wichita, written commun., September 25, 2009) and monthly artificial recharge data for phase I ASR sites for 2007 through 2008 were obtained from the city of Wichita (U.S. Geological Survey, 2011). Monthly pumping rates were

used to calculate an annual rate used for the Wichita wells. The city of Wichita also provided annual artificial-recharge data for 2002 through 2005 for the *Equus* Beds Groundwater Recharge Demonstration sites (U.S. Geological Survey, 2011). Locations for Wichita's production wells and the phase I ASR artificial-recharge wells were provided by KDA-DWR. Locations of the *Equus* Beds Artificial-recharge Demonstration Project recharge sites were those previously determined by the USGS.

The pumping wells and artificial-recharge sites were assigned to the model-grid cell they plotted within based on decimal-degree locations provided by KDA-DWR. Each well was evaluated individually to determine the altitude of the bottom of the well and the screened interval. The top and bottom altitudes were used in the MultiNode Well Package to vertically distribute well pumping across model layers for each well.

The depth of each well was determined using one of the following methods. Where data were available, the altitude of the bottom of the screened interval was used. For unknown screened intervals, the altitude of the bottom of the well was used. If the altitude of the bottom of the screened interval or depth of the well were unknown, and aquifer information provided by KDA-DWR indicated the well was in the *Equus* Beds aquifer, well depth was assigned as the depth of the lowest model layer in the cell that contained the well. If the well was not in the *Equus* Beds aquifer, it was excluded from use.

The top of the screened interval for each well was determined using one of the following methods. If the screened interval was known, the top altitude was used. If the screened interval was unknown, the top of the screened interval was arbitrarily set at 20 ft below land surface. For shallow pumping wells located in model layer 1, the top of the screened interval was arbitrarily set at 10 ft below land surface. Locations of simulated pumping wells for 1980 through 2008 are shown in figure 30.

Industrial pumpage was assumed to be at a constant rate throughout the year. The annual volume of pumpage divided by the number of days in the year was used to calculate a pumpage rate in cubic feet per day.

Two modifications were made to the annual irrigation pumpage data obtained from KDA-DWR. Irrigation pumpage that was unmetered (pumpage reported as the number of hours the pump ran multiplied by a pump rate) was considered over-reported and was reduced by varying annual percentages. Comparisons of pumpage at selected wells before and after metering indicated that unmetered pumpage was over-reported by about 20 percent before 1990 (Andy Lyon, Kansas Department of Agriculture, Division of Water Resources, written commun., July 2010). The KWO estimates the percentage by which the annual reported unmetered irrigation water is greater than actual irrigation (Kansas Water Office and Kansas State Board of Agriculture, Division of Water Resources, 1989) using the following equation:

Table 5. Estimated return flow from irrigation by irrigation system types.

[KDA-DWR, Kansas Department of Agriculture–Division of Water Resources]

Return-flow system type	Estimated return flow (percent)	KDA-DWR irrigation system type
Flood	25	Flood
Center-pivot high-impact nozzle	9	Unreported Center pivot-standard Sprinkler other Other
Center-pivot low-impact drop nozzle	7	Drip Center-pivot low-impact drop nozzle Drip and other
Combination	12.2	Center pivot and flood (assumed 80-percent center-pivot-standard and 20-percent flood)

Some of the Wichita production wells were redrilled, causing substantial changes in screen and well depths. Information from NWIS and Wichita (Rich Robinson, city of Wichita, written commun., December 2009) about the well and screen depths, and information available from KDA-DWR was used to more accurately assign well and screen depth for each well in each stress period.

Annual volumes of artificial recharge in gallons for the *Equus* Beds Demonstration Recharge sites and at each of the phase I ASR sites (U.S. Geological Survey, 2011) were available. These volumes were converted to cubic feet and then divided by the total number of days in the year to get the artificial-recharge rate in cubic feet per day as used in the model.

Some of the *Equus* Beds Recharge Demonstration and phase I ASR project's artificial-recharge sites that are not wells (for example, basins or trenches; fig. 3) cover parts of adjacent model-grid cells; however, all of the artificial recharge for these sites was assigned to the cell that contained the point location previously used as the location of the site. The error associated with assigning artificial recharge to one cell instead of all the cells that intersect the recharge basins is assumed to be small because the recharge basins do not extend more than one cell from the point location previously used as the location of the site. Because the model treats sites where water is pumped into or out of the aquifer as wells, the artificial recharge was distributed to the entire cell. If recharge wells were drilled into a recharge basin (for example, at the Recharge Demonstration basins at Halstead) and the amount of recharge at each well was unavailable, the total amount was divided equally among them.

Head-Dependent Boundaries

The *Equus* Beds aquifer extends beyond the model boundary in several areas, and thus the model boundary does not represent the actual physical or groundwater flow boundaries of the aquifer. These boundaries were simulated in

the model as general head boundaries, a form of the head-dependent flux boundary that allows groundwater to enter or exit the model proportional to the difference between the water level in the model and the water level assigned to the boundary multiplied by a conductance term that limits the rate of flow (McDonald and Harbaugh, 1988). These boundaries were located as far as practical from the Wichita well field to limit boundary effects on model results. Water levels along the boundary were assigned to each general head boundary cell based on an assumed water table value located 20 miles outside the model. General head boundary conductances were calculated by multiplying the hydraulic conductivity of each general head boundary cell by the length and width of the cell divided by the distance to the location of the assumed water-table value (20 miles). General head boundaries are shown in figure 31.

Head and Streamflow Gain and Loss Observations

Groundwater-level observations and streamflow gain and loss observations were compared to simulated groundwater levels and streamflow gains and losses using the Head Observation Package and the River Observation Package (Harbaugh and others, 2000) for the steady-state and transient groundwater calibration simulations. Groundwater-level observation data, including groundwater level altitude, well location within the model, and time of observation, were calculated and entered into the Head Observation Package.

Groundwater-level data and associated well-construction and aquifer information available from the USGS NWIS database (U.S. Geological Survey, 2009a; U.S. Geological Survey, unpub. data, 2009) and the Kansas Geological Survey's WIZARD database (Kansas Geological Survey, 2009) were compiled for wells in the study area. Groundwater levels commonly are recorded as depth below land surface. To convert them to groundwater altitudes, they were subtracted from the land-surface altitude determined for the well. If a land-surface altitude was not determined for the well, one was estimated

from the National Elevation Datum database (U.S. Geological Survey, 2009b). Wells and their associated groundwater altitudes were assigned to a model layer based on the altitude of the bottom of the well's screened interval, or, if the screened interval was unavailable, the altitude of the bottom of the well. If neither of these data values were available, then the well was not used. Hydrogeologic information stored in NWIS was used to confirm that a well was open to the *Equus* Beds aquifer. If a well was in the aquifer but was 5 or fewer ft deeper than the bottom of the modeled aquifer, the well was retained in the dataset and the water-level altitude assigned to the bottom layer of the model.

Streamflow gain or loss observation data, including a list of model cells for each stream reach and flow into or out of the aquifer along the stream reach, and time of observation were calculated and entered into the River Observation Package. Streamflow measurements at USGS streamflow gages on the Arkansas River near Maize (07143375) and Hutchinson (07143330), and on Little Arkansas River at Valley Center (07144200) and Alta Mills (07143665) (fig. 6) were used to estimate base flow (gains from and losses to the aquifer) for each model stress period when measurements from each pair of gages were available using hydrograph separation (Lim and others, 2005). Mean base flow for each stress period was calculated for each gage. Streamflow gains and losses for each stress period were then calculated by subtracting upstream gage base flow from downstream gage base flow. Streamflow gain is caused by discharge of water from the aquifer to the stream and is represented by a negative number. Conversely, streamflow loss results from water flow from the streams into the *Equus* Beds aquifer and is represented by a positive number.

Geometric Multigrid Solver

The groundwater flow equation was solved by the geometric multigrid method (Wilson and Naff, 2004), a method for solving the groundwater flow equation. Closure criteria are set to stop the iterative solver for head and flow residual. The head closure criterion was set to 0.01 ft and the flow residual criterion was set to 1,000.0 ft³/day.

Model Calibration

The groundwater-flow model was calibrated by adjusting model input data until model results matched field observations within an acceptable level of accuracy (Konikow, 1978). Both steady-state and transient hydraulic head and streamflow data were used to calibrate the model. Steady-state conditions occur when inflow to the system equals outflow from the system. Calibration to steady-state conditions was used to assess the conceptual model of groundwater flow and simulated boundary conditions, and estimate hydraulic conductivity values and recharge rates. Transient conditions occur when inflow does not equal outflow and is balanced by water flow

into or out of the aquifer from storage. Calibration to transient conditions refined the model hydraulic properties determined from the steady-state calibration and provided estimates of storage properties of the aquifer.

Calculation of parameter sensitivities was used for the steady-state predevelopment simulation to indicate the relative importance of each model input variable. Parameter values from the steady-state simulation were used as a starting point for manual calibration of the transient simulation. Hydraulic properties adjusted during the calibration process include horizontal hydraulic conductivity, vertical hydraulic conductivity between model layers, specific storage, specific yield, recharge rates, evapotranspiration, streambed hydraulic conductivity, and general head boundary conductance. After each change in one of these parameters, the simulated groundwater levels and streamflow gains and losses were compared to observed values. The difference between simulated and observed values is called the residual. Parameter estimation (Harbaugh and others, 2000) was attempted for the transient simulation; however, nonconvergence for the transient parameter-estimation simulations prevented its use. The nonconvergence was most likely caused by nonlinear groundwater flow, heterogeneous hydraulic properties of the *Equus* Beds aquifer, and complexity of the transient simulation.

The model accuracy was estimated using several methods. The root mean square (RMS) error between observed and simulated hydraulic head as well as observed and simulated streamflow gains or losses were calculated for each well and stream observation for the entire simulation. Model accuracy was increased by minimizing the RMS error during the calibration process. The RMS error measures the absolute value of the variation between measured and simulated hydraulic heads at control points or the variation between measured and simulated streamflow along stream reaches. The equation to calculate the RMS error is:

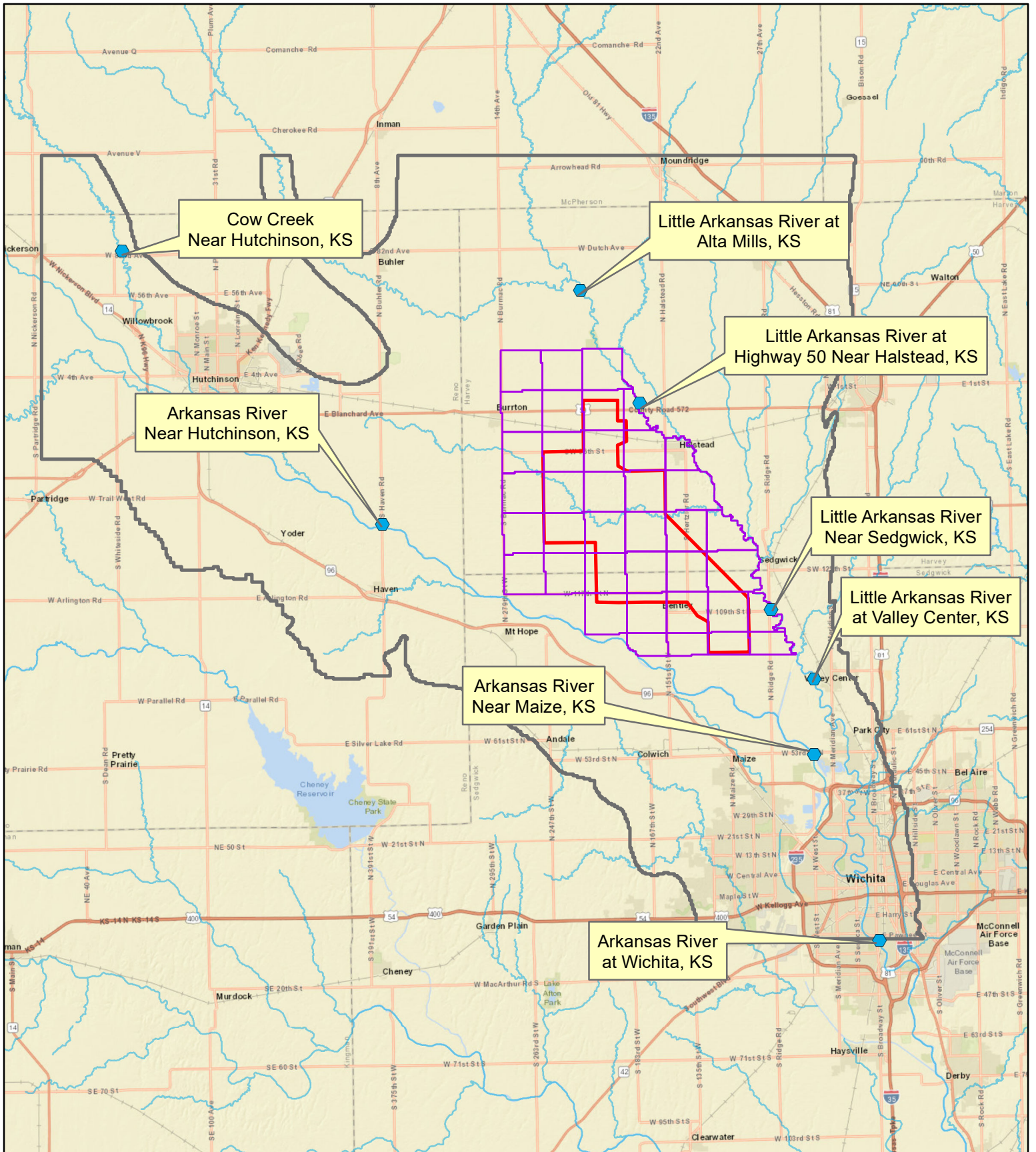
$$\text{RMS error} = \sqrt{\frac{e_1^2 + e_2^2 + e_3^2 + \dots + e_n^2}{n}}, \quad (5)$$

where




- e is the difference between the observed and simulated values, and
- n is the number of observations.

Water-table altitudes range from about 1,500 to about 1,300 ft above NAVD 88 in the main part of the model area between Hutchinson and Wichita, Kans. (or 200 ft of head loss, excluding the dune sand area) (Myers and others, 1996). The ratio of the RMS error to the total head loss in the model area is a measure of the amount of model error in the overall model response. A value less than 10 percent is a generally accepted threshold (Anderson and Woessner, 1992). Thus, for this study, the RMS error divided by the total head loss should be less than 20 ft (10 percent of the 200 ft of head loss in the model area).

The mean error between observed and simulated hydraulic head and between observed and simulated streamflow gains



Legend

-  USGS Stream Gaging Station
-  ASR Index Cells & Basin Storage Area)
-  USGS Central Wellfield Study Area
-  Boundary of Active Groundwater Model



1:400,000

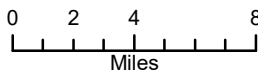


Figure 4
USGS Stream
Gage Stations
Utilized in EBGWM

The ratio of horizontal hydraulic conductivity to vertical hydraulic conductivity within model layer 1 ranges from 10 to 500 and is shown in figure 24. Larger values indicate smaller vertical hydraulic conductivity. Small vertical hydraulic conductivity values were assigned to account for vertical anisotropy caused by thin layers of clay, silt, and fine-grained sand in parts of the study area (Myers and others, 1996). The ratio of horizontal hydraulic conductivity to vertical hydraulic conductivity between adjacent cells within model layers 2 and 3 was set at 10 to account for vertical anisotropy caused by thin layers of clay, silt, and fine-grained sand.

A specific yield of 0.15 was used for model layers 1, 2, and 3 to represent conditions where water is released from storage as water drains from the aquifer. A storage coefficient of 0.0005 was used for model layers 1, 2, and 3 to represent conditions where water is released from storage because of expansion of the water or compaction of the aquifer material and not actual drainage of water from the aquifer. All model layers were defined in MODFLOW-2000 as convertible and each required a specific yield and a confined storage coefficient value as model input.

Boundary Conditions

Model boundary conditions are used to specify flow into and out of the model domain. Sources of flow into and out of the aquifer include recharge, evapotranspiration, gaining and losing streams, pumping wells, and artificial recharge wells and basins. The groundwater-flow model simulates the water table as a free surface, where its position is not fixed but varies with time (Franke and others, 1984). Specified flux boundaries, where the volume of water that flows across the boundary is a function of time, position, and head, and varies as a function of flow, include the lateral boundary of the *Equus* Beds aquifer, bedrock (no flow boundaries), and recharge from precipitation. Head-dependent flux boundaries where water flow varies as a function of head and conductance include flow across lateral boundaries of the model, evapotranspiration, gaining and losing streams, pumping wells, and artificial recharge wells and basins.

Recharge

The water table is the surface across which areally distributed recharge enters the aquifer. Recharge to the model was applied to the top-most active cell in each vertical column and varied temporally as a function of average precipitation for each stress period and spatially as a percentage of precipitation.

Annual precipitation data for 1938 through 2008 for six Cooperative and Weather Bureau Army Navy (WBAN) weather stations in and near the study area were used to estimate the precipitation for the study area. Average precipitation for each stress period and periods of data from weather stations used in the model are listed in table 3 at the back of this

report. Average annual precipitation for weather stations near the Wichita well field is shown in figure 25. Average precipitation calculated from weather stations was evenly distributed across the model for each stress period.

The areal distribution of soil permeability (Juracek, 2000) was used for the initial distribution of recharge rate as a percent of rainfall. Soil permeability was divided into six groups shown in figure 26. Soils with low permeability were assigned small values of recharge as a percent of precipitation and soils with large permeability were assigned large values. The initial distribution of recharge as a percent of precipitation was altered during the course of model calibration to more closely match simulated and observed groundwater levels. The final distribution of recharge as a percentage of precipitation for each recharge zone is shown in figure 27.

Evapotranspiration

Evapotranspiration is simulated in the model as removal of water from the saturated aquifer through plant transpiration and evaporation. Evapotranspiration is set to a maximum rate when the water table is at land surface and is set to zero (extinction depth) when the water table is more than a specified depth below the land surface (set at 10 ft). Evapotranspiration varies linearly with changes in the water table between the two surfaces. Maximum average evapotranspiration was calculated for each stress period using the Hamon equation (Hamon, 1961; Alkaeed and others, 2006). The Hamon equation uses only saturated vapor pressure, mean daily air temperature, and average number of daylight hours per day as input. Evapotranspiration was estimated for 1935 through 2008 using mean monthly air temperature and saturation vapor pressure from the Cooperative Weather Station at Newton, Kans. (station 145744). Daily values of maximum evapotranspiration were used to calculate evapotranspiration for each stress period in feet/day. The Hamon equation is:

$$ET_o = \frac{2.1H_t^2 e_s}{(T_{mean} + 273.2)} \quad (2)$$

where

- ET_o is the evapotranspiration for the stress period,
- H_t is the average number of daylight hours per day for the stress period,
- e_s is the saturation vapor pressure in millimeters per day at the mean daily air temperature for the stress period, and
- T_{mean} is the mean daily air temperature (°C) for the stress period.

and

$$e_s = 6.112 \cdot \exp[17.67 \cdot (T)/(T+243.5)] \quad (3)$$

where

- T is the mean daily air temperature for the stress period (Rogers and Yau, 1989).

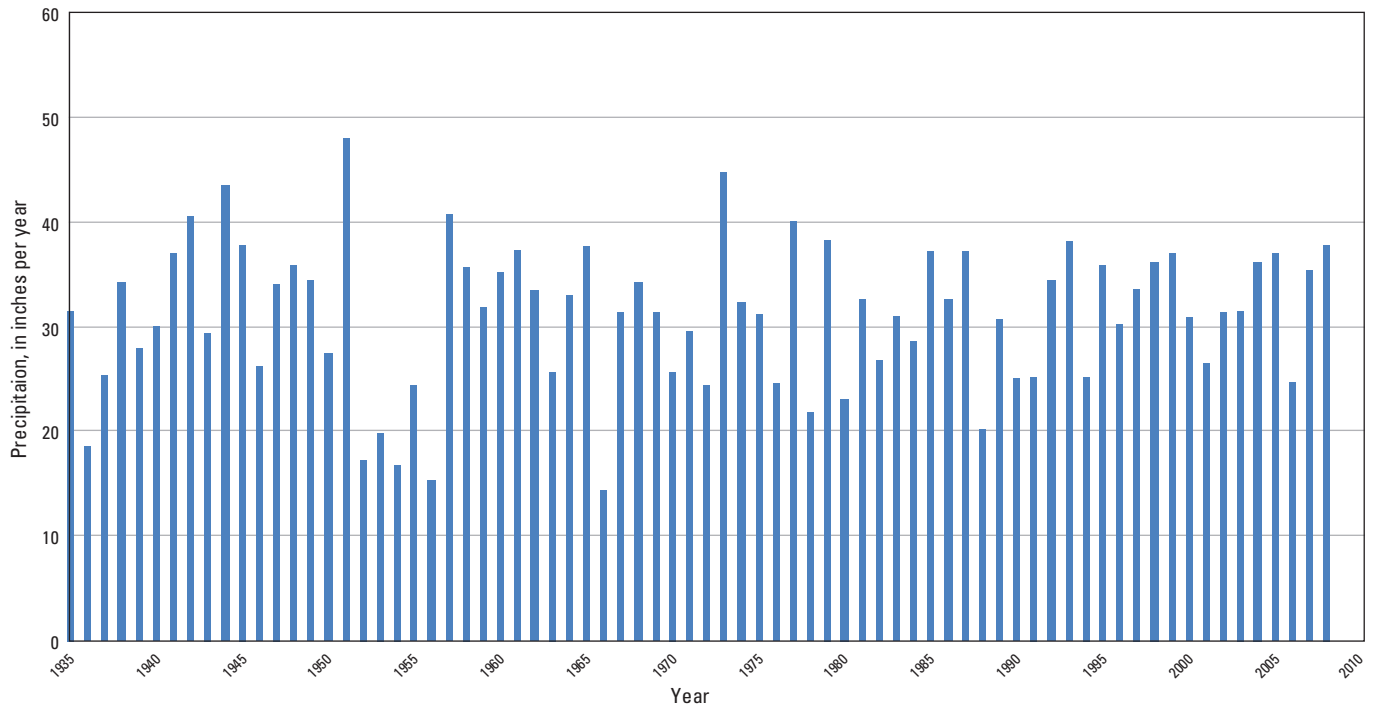


Figure 25. Average annual precipitation in inches per year for weather stations at Hutchinson (143930), Mt. Hope (145539), Newton (145744), Sedgwick and Halstead (143366) and Wichita (148830) near the Wichita well field (National Oceanic and Atmospheric Administration, 2008).

The average number of daylight hours per day was calculated for a point near the center of the model area, at Halstead, Kans. (longitude 97°31'00" W, latitude 38°00'00" N). Sunrise and sunset times were obtained from the Astronomical Applications Department, U.S. Naval Observatory (http://aa.usno.navy.mil/data/docs/RS_OneYear.php). Temperature data from Newton, Kans. were used for the computation because a complete record was available from National Climate Data Center Archives (<http://lwf.ncdc.noaa.gov/oa/climate/stationlocator.html>). Initial estimated evapotranspiration was altered during calibration to more closely match observed and simulated groundwater levels.

Streams

The Arkansas River, Little Arkansas River, and their tributaries are represented in the model as head-dependent flux boundaries. The Arkansas River, Little Arkansas River, and Cow Creek (near Hutchinson, Kans.) were simulated in MODFLOW-2000 using the River Package and the smaller streams and tributaries were simulated using the Drain Package (McDonald and Harbaugh, 1988). All rivers and drains are within model layer 1.

Flow into or out of the aquifer at each of the cells where a river is simulated is a function of the river stage with respect to the altitude of the potentiometric surface, the hydraulic conductivity of the streambed material, the cross-sectional area of flow between the stream and the aquifer, and the altitude of the water table with respect to the altitude of the

streambed (McDonald and Harbaugh, 1988). Stream stages in the Arkansas and Little Arkansas Rivers were recorded at streamflow gages (fig. 6) hourly (U.S. Geological Survey, 2009a) and average annual stage was calculated for each gage. The average annual altitude of the river surface used in each stress period of each simulation was assigned to each model cell with a stream by interpolating the specified river surface altitude between gaging stations. Each stream was assigned a single value for streambed hydraulic conductivity. The area of the stream within each model cell was calculated and the streambed hydraulic conductivity value was multiplied by the area of the stream and then divided by the thickness of the streambed to determine the streambed conductance. Streambed thicknesses are unknown and were assigned an arbitrary value of 1 ft. Initial streambed conductances were altered during calibration to more closely match observed and simulated flow between the streams and the aquifer.

Flow into or out of the aquifer at each of the cells where a drain is simulated is a function of the altitude of the potentiometric surface, the hydraulic conductivity of the drain bed material, the cross-sectional area of flow between the drain and the aquifer, and the altitude of the water table with respect to the altitude of the drain bed (McDonald and Harbaugh, 1988). Each stream simulated as a drain was assigned a single value for streambed hydraulic conductivity. The area of the stream within each model cell was calculated and the initial streambed hydraulic conductivity value was multiplied by the area of the stream and then divided by the thickness of the streambed to determine the streambed conductance.

within the BSA as a percentage of predevelopment saturated thickness (Figure 9). By contrast, at the end of the 8-year simulated drought, the average remaining saturated thickness as a percentage of predevelopment saturated thickness was 86% for model cells in the CWSA and 89% for model cells for the entire BSA (see Figure 10 and Table 2-9).

Table 2-9: Groundwater Modeling Results for 1% Drought Simulation

EBGWM 1% Drought Simulation Statistics	Drought Years								Recovery Years	
	SP1	SP2	SP3	SP4	SP5	SP6	SP7	SP8	SP9	SP10
ASR BSA avg Water Level Change from Starting Conditions (ft)	-1.8	-3.4	-5.2	-6.1	-7.3	-7.7	-7.9	-8.2	-6.1	-4.6
CWSA avg Water Level Change from Starting Conditions (ft)	-2.1	-4.4	-7.7	-8.9	-11.0	-11.2	-11.4	-11.6	-8.6	-6.3
ASR BSA Aquifer Condition (% Full)	93%	92%	91%	90%	90%	90%	90%	89%	91%	91%
CWSA Aquifer Condition (% Full)	90%	89%	87%	87%	86%	86%	86%	86%	87%	88%

Hydrographs have been generated for the model cells belonging to each of the existing ASR Index Well (IW) sites to record simulated water levels (Attachment I - Hydrographs 1 through 38). Further review of the hydrographs relative to January 1993 aquifer conditions indicates that groundwater levels within the EBWF are projected to fall below the current ASR minimum index levels during the simulated drought. Tables and maps illustrating when and where the January 1993 conditions are encountered have also been included within Attachment I.

2.6 Proposed Modifications to ASR Minimum Index Water Levels

The results of EBGWM 1% drought simulation confirm that after the drought, pumping demands will cause groundwater levels within the majority of the EBWF to drop below the currently permitted ASR minimum index level restrictions (Attachment I). This requires the City to seek reasonable alternative minimum index water levels for the existing ASR project that ensure recharge credits are available throughout periods of drought. The results of the EBGWM 1% drought simulation were utilized to calculate the lowest groundwater elevation for each IW site throughout the eight-year simulated drought.

Table 2-10: Development of Proposed ASR Minimum Index Levels

Index Well No.	Minimum Drought Model Elevation (feet)	Minimum Index Level Elevations			
		Existing Level (1993 Level) (feet)	Basis for Proposed Level ¹	Contingency Added (feet)	Proposed Levels ² (feet)
IW01C	1429.14	1413.42	Existing	20	1390
IW02C	1407.96	1410.52	Existing	10	1390
IW03C	1389.76	1396.93	Modeled	10	1380
IW04C	1420.35	1417.6	Existing	10	1407
IW05C	1408.21	1407.23	Modeled	10	1398
IW06C	1380.42	1388.74	Modeled	10	1370
IW07C	1372.79	1369.95	Existing	10	1360
IW08C	1418.06	1417.56	Modeled	10	1408
IW09C	1394.74	1394.1	Modeled	10	1385
IW10C	1368.08	1375.09	Modeled	10	1358
IW11C	1365.27	1363.75	Existing	10	1354
IW12C	1370.6	1365.78	Existing	10	1355
IW13C	1417.21	1418.27	Modeled	10	1407
IW14C	1386.6	1396.56	Modeled	10	1377
IW15C	1364.07	1369.75	Modeled	10	1354
IW16C	1354.11	1360.21	Modeled	10	1344
IW17C	1363.16	1360.59	Existing	10	1351
IW18C	1417.28	1421.4	Modeled	10	1407
IW19C	1396.07	1398.95	Modeled	10	1386
IW20C	1373.34	1376.05	Modeled	10	1363
IW21C	1352.12	1363.04	Modeled	10	1342
IW22C	1353.79	1354.92	Modeled	10	1344
IW23C	1356.94	1355.55	Existing	10	1345
IW24C	1416.31	1418.96	Modeled	10	1406
IW25C	1403	1407.27	Modeled	10	1393
IW26C	1380.64	1374.89	Existing	10	1364
IW27C	1363.16	1360.92	Existing	10	1350
IW28C	1343.8	1349.14	Modeled	10	1334
IW29C	1350.36	1349.51	Modeled	10	1340
IW30C	1386.13	1379.77	Existing	10	1370
IW31C	1376.18	1366.06	Existing	10	1356
IW32C	1362.86	1356.51	Existing	10	1346
IW33C	1348.93	1344.68	Existing	10	1334
IW34C	1344.62	1344.24	Modeled	10	1335
IW35C	1373.74	1366.76	Existing	10	1356
IW36C	1363.02	1360.13	Existing	10	1350
IW37C	1352.85	1350.51	Existing	10	1340
IW38C	1343.19	1344.65	Modeled	10	1333

¹ Existing refers to the Existing 1993 Level, Modeled refers to the Minimum Drought Model Elevation.

² Values were rounded to the nearest foot.



August 21, 2019

Brian McLeod
Deputy City Attorney
City of Wichita
455 N. Main, 13th Floor
Wichita, KS 67202

Re: Review of ASR Permit Modification Expert Report submitted by
Masih Akhbari, PhD, PE

Introduction and Purpose

Burns & McDonnell has been retained by the City of Wichita (City) to provide expert witness hearing testimony in the matter of the City's ASR Permit Modification Proposal (Proposal). Also, at the request of the City a review and critique of the technical expert report submitted by Masih Akhbari, PhD, PE has been completed and summarized below:

Review of the Expert Report submitted by Masih Akhbari, PhD, PE

Expert Report, page 8 – *The USGS report uses Root Mean Square (RMS) error as the metric to evaluate model calibration. RMS error is a measure to take an average of the differences between the observed and simulated data values over time and space in this case. To elaborate, when and where observed data have been available, the difference between the observed and simulated values has been calculated and squared. Then, these squared differences for all timesteps with observed data and at all monitoring wells have been averaged and the root of this value has been calculated as the RMS error. Clearly, such average offsets the highly over- or under-estimated simulation values by balancing them out with when or where the errors is low. According to the USGS report, the RMS error for water-levels of the transient calibration of the EBGWM is 2.48 ft, indicating “the acceptability of the calibrated model,” as stated in Page 48 of the USGS report. However, more detailed comparison between simulated and observed values indicates that the model tends to mainly underestimate water levels across the 20 selected monitoring wells shown in Figure 34 of the USGS report. I provided a copy of this figure at the end of this report (Figure 3).*

The RMS error represents the average error in a model and is a statistical parameter used to quantitatively evaluate the “goodness of fit” of a model. Statistical parameters quantify model calibration goals and establish the maximum acceptable average error in the model. For the EBGWM, the USGS established that a RMS error, normalized against the total head change within the model, should be less than 10 percent (USGS SIR2013-5042 page 46) “A value less than 10 percent is a generally accepted threshold (Anderson and Woessner, 1992).”. In the transient model, the USGS provides the following calibration summary (USGS SIR 2013-5042 page 83): “The RMS error for all water-level observations for the transient calibration simulation is 2.48 ft. The ratio of the RMS error to the total head loss in the model area is 0.0124 (2.48 ft divided by 200ft) or 1.24 percent.”.

As summarized above, the normalized RMS error in the transient model calibration is well below accepted thresholds for groundwater model calibration. For a model like the EBGWM, where the ratio of the RMS effort to the total head in the model is low, the model errors are “only a small part of the overall model response” (Anderson and Woessner, 1992 page 241). The full quote from the model report concludes “acceptability of the calibrated model” based on both RMS error and the potential

Brian McLeod
City of Wichita
August 21, 2019
Page 2

measurement error within the calibration dataset. USGS SIR 2013-5042 page 45 “Wells were selected to include all model layers and a wide distribution in the model. A total of 3,677 water-level observations from 1935 through 2008 were used for the transient calibration. The RMS error for all water-level observations is 2.48 ft for the transient calibration. This value is less than the maximum measurement errors and indicates the acceptability of the calibrated model.”

The statement that a comparison between the simulated and observed water level elevations across the 20 monitoring wells “mainly underestimates water level across the 20 selected monitoring wells shown in Figure 34 of the USGS report” ignores the transient hydrographs provided in the USGS report, immediately following Figure 34 (USGS SIR 2013-5042 pages 58 -65). These hydrographs illustrate the temporal variability of water levels (both observed and simulated) and highlight the model’s ability to track transient changes in groundwater levels within the model domain over time.

Expert Report, pages 8 and 9 - I downloaded the simulated and observed water levels in selected monitoring wells from Table 9 of the USGS report, listed on Page 89 of this report, and provided a summary of my analysis in Table 3. According to this table:

While the RMS error seems to be low, comparing the total range of water level changes over the entire observation period (Column C) with the maximum and average differences between observed and simulated values (Columns D and E, respectively) suggests that the error should be taken into account more seriously. For example, at monitoring well #741, water levels fluctuate about 8.21 ft over the period of 1952 to 2008 (Column B). The maximum and average differences between the simulated and observed water levels are 4.95 ft and 3.03 ft, respectively, which correspond to 60% and 37% of the total range of long-term water level fluctuations (Columns F and G, respectively). The averages of these ratios, presented in Columns E and F, over all 20 wells are 68% and 31%, respectively.

The period of record used to calibrate the transient groundwater model is almost 70 years for many of the observation wells. While the error between observed and simulated water level elevation over this 70-year period does often vary by year, the average absolute difference (Column E in Expert Report Table 3) for all observation wells is 2.1 feet. As with all model statistical parameters, the model error must be evaluated over the total head change within the model area to provide the proper context for that model simulation. Given the 200-foot head difference within the EBGWM model, this average absolute error equates to a normalized average absolute error of 1.1%. This low error, along with the water level trends shown on the transient hydrographs provided in the USGS report (USGS SIR 2013-5042 pages 58 -65), illustrate that the USGS groundwater model reasonably approximates both spatial and temporal water level changes within the aquifer over the 70-year calibration period.



Brian McLeod
City of Wichita
August 21, 2019
Page 3

Expert Report, page 10 - *Item 2 in the Model Limitations Section of the USGS report (Page 72) explicitly states that “The groundwater-flow model was discretized using a grid with cells measuring 400 ft by 400 ft. Model results were evaluated on a relatively large scale and cannot be used for detailed analyses such as simulating water-level drawdown near a single well. A grid with smaller cells would be needed for such detailed analysis.” However, as presented in Table 2-10 of the ASR Permit Modification Proposal, minimum Drought Model elevations at the location of Index Wells have been used to propose modified ASR Minimum Index Levels for more than half of these wells. A copy of this table is provided at the end of this report (Table 4).*

Using the quote from the USGS report the Expert Report mistakenly asserts that the model cannot predict water levels at any point within a model cell. Several MODFLOW post processing utilities exist that calculate the water level within any point of a model cell based on the hydrogeologic properties within that specific cell (for example, see USGS Open File Report 96-651A).

Extrapolated water level elevations were not used to develop Table 2-10 of the ASR Permit Modification Proposal, as suggested by the Expert Report. The minimum drought model elevations supplied in Proposal Table 2-10 are the elevation of the predicted water level for the center of the MODFLOW model cell that overlaps the geographic location of each index well location.

Burns & McDonnell appreciates the opportunity to be of service to the City. Should you have any questions on the review of the Expert Report please feel free to contact me directly.

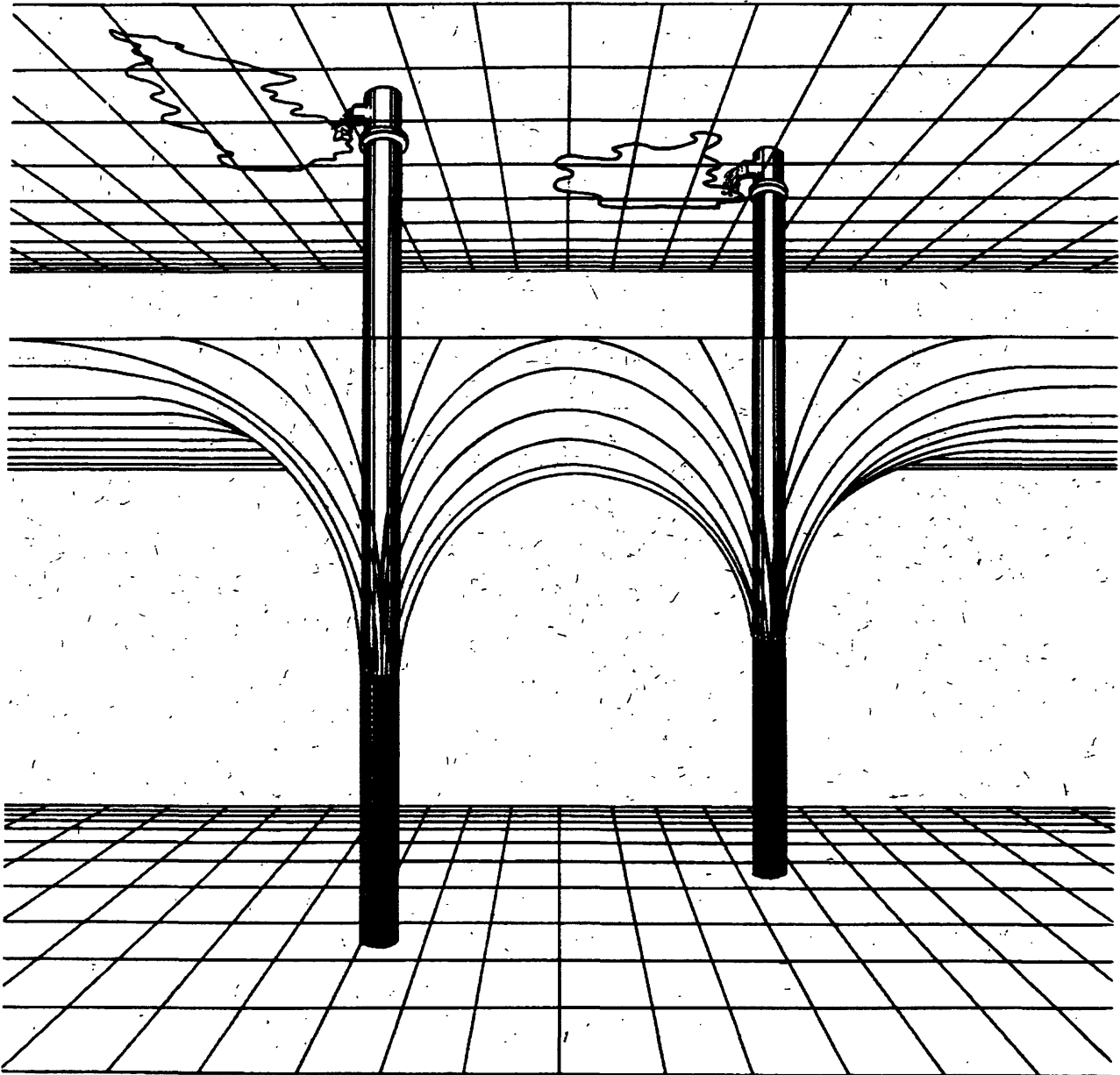
Sincerely,

Luca DeAngelis, P.E.
Associate Geological Engineer

LD/ld

Attachment – USGS Open File Report 96-651-A

Documentation of a Computer Program to Estimate the Head in a Well of Finite Radius Using the U.S. Geological Survey Modular Finite Difference Ground-Water Flow Model



U.S. DEPARTMENT OF THE INTERIOR
BRUCE BABBITT, Secretary

U.S. GEOLOGICAL SURVEY
Gordon P. Eaton, Director

Any use of trade, product, or firm names in this publication is for descriptive purposes only and does not imply endorsement by the U.S. Geological Survey.

For additional information
write to:

District Chief
U.S. Geological Survey
Suite 3015
227 N. Bronough Street
Tallahassee, FL 32301

Copies of this report can be
purchased from:

U.S. Geological Survey
Branch of Information Services
Box 25286
Denver, CO 80225

Documentation of a Computer Program to Estimate the Head in a Well of Finite Radius Using the U.S. Geological Survey Modular Finite Difference Ground-Water Flow Model

By Michael Planert

Contents

Abstract	1
Introduction	2
Theoretical Development of Computation of Head in a Pumping Well of Finite Radius	2
Comparison of Simulated and Analytical Results	4
Program Design	4
Description of Subroutine WELHPW	5
Input for Well Package	7
Sample Input	8
Sample Output	9
References	11

Figures

1. Flow from cell $(i-1, j)$ to cell (i, j) and equivalent radial flow to well (i, j) with radius r	3
2. Program structure	6

Tables

1. Analytical results for pumping well used to test equation 4	4
2. Comparison of analytical results to simulated results using equation 4 for varying grid dimensions and two values of transmissivity	5

Abstract

The **hdpw** (head-in-a-pumping-well) program described in this report is a post-processor that calculates the head in a pumping well based on the simulated head at a finite-difference model cell that contains the well. The calculations are based on the Thiem equation. The **hdpw** code works with the U.S. Geological Survey modular finite-difference ground-water flow model, which is commonly called MODFLOW. The **hdpw** code is a complete program that has incorporated many of MODFLOW subroutines to read data. Code was added to the well package to calculate the head and drawdown in a fully penetrating well of finite radius.

Introduction

A finite-difference model does not calculate an accurate value for a head in a pumping well when the grid dimension is larger than the well diameter. The model-calculated value of head is usually higher than the actual value for a pumping well and lower than the actual value for an injection well. Prickett (1967) has shown that the head in a square model cell containing a pumping well could be related to a radius (termed effective radius by Prickett) of approximately 0.21 times the cell dimension in which a well resides. The values of the head calculated for the cell and the effective radius for the cell can be used in the Thiem equation to estimate what the head would be in an actual well having a much smaller diameter.

The program described in this report can be used with MODFLOW to compute the head and drawdown in a well of a finite radius. Calculating an approximate head for a pumping well allows a better evaluation of the production capabilities of the aquifer and of designs to remediate ground-water contamination. Also, the program might allow better evaluation for areal studies when only pumping levels are available for production wells that would be the calibration criteria for these flow models.

Copies of the computer program are available through the World-Wide Web at address:

<http://h2o.usgs.gov/software/>

Copies of the computer program are also available on diskette for the cost of processing from:

U.S. Geological Survey
NWIS Program Office
437 National Center
Reston, VA 20192
Telephone (703)648-5695

Theoretical Development of Computation of Head in a Pumping Well of Finite Radius

The following discussion is based on pages 8 to 10 of Trescott and others (1976). The hydraulic head computed at a cell containing a well represents the average hydraulic head for the entire cell and is not the head in the well.

Prickett (1967) has shown that the effective radius, r_e , for the average head for a model cell can be determined from the cell dimensions, when $\Delta x = \Delta y$, by the equation

$$r_e = r_1/4.81, \quad (1)$$

where $r_1 = \Delta x = \Delta y$.

The routine to calculate the head in a well is based on the Thiem (1906) equation which assumes steady flow, no stress term other than the well discharge, and that the area around the well is isotropic and homogeneous. The derivation of equation 1 is from the combination of equations written for planar flow to a model cell with a pumping well and radial flow to a well. Figure 1 depicts a model cell with a pumping well in planar and radial coordinates. The equation can be simplified by considering only two dimensions where the cell i,j is surrounded by four cells. Assuming that these cells have equal head values, all sides of the model cell will receive the same discharge. Figure 1a depicts one-quarter of the discharge to the well node i,j computed by the model as

$$Q_{w(i,j)}/4 = \Delta x_j T_{i,j} (\Delta h/\Delta y), \quad (2)$$

where $\Delta h = h_{i-1,j} - h_{i,j}$ and

$$T_{i,j} = T_{xx(i,j)} = T_{yy(i,j)}.$$

An equivalent equation can be written for radial flow to a well using the Thiem (1906) equation, as shown in figure 1b:

$$Q_{w(i,j)}/4 = [\pi T_{i,j}/2] [\Delta h/\ln(r_1/r_e)]. \quad (3)$$

Equation 1 can be obtained from equating the discharges in equations 2 and 3.

The Thiem equation is further used to extrapolate from the head, $h_{i,j}$, for the model cell at the effective radius, r_e , to the head, h_w , at the desired well radius, r_w . The equation is written

$$h_w = h_{i,j} - [Q_{w(i,j)}/2\pi T_{i,j}] \ln(r_e/r_w). \quad (4)$$

Assumptions for equation 4 are:

1. The aquifer is confined.
2. The well causes radially symmetric drawdown.
3. The well causes no vertical flow in the aquifer containing the well or from units above and below the aquifer.
4. The transmissivity is uniform and isotropic in the cell containing the well and the four neighboring cells.
5. The grid dimensions for the cell containing the well and the four neighboring cells are uniform.
6. The well is pumping under steady-state conditions.
7. There are no head-dependent conditions nearby.
8. The well is 100 percent efficient.

The analogous equation for an unconfined aquifer is written as:

$$H_w = \sqrt{H_{i,j}^2 - [Q_w(i,j)/\pi K_{i,j}] \ln (r_e/r_w)}, \quad (5)$$

where

$H_{i,j} = h_{i,j} - \text{BOTTOM (I,J)}$ is the saturated thickness of the aquifer at radius r_e (L);
 H_w is the saturated thickness of the aquifer at the well (L);
 $K_{i,j} = K_{xx(i,j)} = K_{yy(i,j)}$; is the hydraulic conductivity for the cell;
 BOTTOM (I,J) is the elevation of the bottom of the aquifer.
 (The uppercase letters indicate that this parameter is identical to that used in the model.)

Additional assumptions for unconfined conditions are:

1. Rather than the aquifer having uniform transmissivity, the aquifer bottom is flat in the region and the hydraulic conductivity is uniform and isotropic.
2. There are no other stresses in the cell containing the well or in the four neighboring cells.

3. The saturated thickness of the aquifer is virtually equal at the cell containing the well and in the four neighboring cells.

There is a possibility that the aquifer may become dewatered at the well, r_w , even though it is not dewatered at the effective radius, r_e , for the cell. This condition is indicated in equation 5 when the value calculated beneath the square root symbol is negative. For this condition, the output in the

well table is "WELL IS DRY." If this occurs while actual measurements are being simulated, a review of the transmissive properties and radius used for the well should be made, as most wells are not 100 percent efficient and the aquifer should not go dry. If a well goes dry while determining prospective rates for a pumping system then, obviously, the rates should be lowered.

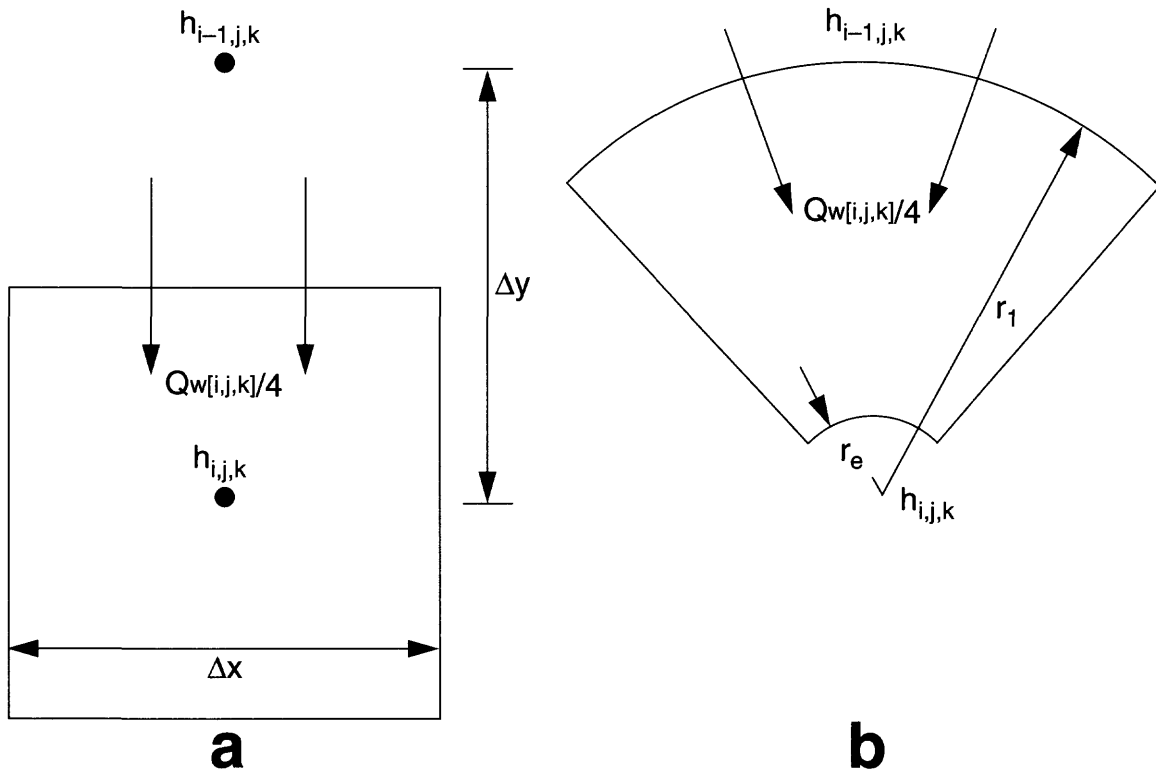


Figure 1. Flow from cell $(i-1,j)$ to cell (i,j) (a) and equivalent radial flow to well (i,j) with radius r , (b). (From Trescott and others, 1976.)

Comparison of Simulated and Analytical Results

To test the accuracy of equation 4, model runs were made to compare to an analytical solution using the Theis equation (1935) assuming steady conditions were attained near the well at the end of the time period simulated. Two models, one using a transmissivity of 500 ft²/d and the other a transmissivity of 5,000 ft²/d, were constructed with a pumping well at the center of the grid, a storage coefficient of 0.0001, and a pumping rate of 10,200 ft³/d. The test actually compares drawdowns, so the initial head was set to zero and the heads calculated were negative and equivalent to the absolute values of the analytical drawdowns. The derivation of equation 4 is based on square grid cells but the code is written to accommodate rectangular grid cells. Different grid dimensions were used to test the error that rectangular grid cells might introduce into the calculated head. As cell dimensions were changed from 100 by 100 ft cells

to 150 by 100 ft cells to 200 by 100 ft cells to 500 by 100 ft cells, the grid dimensions changed with the number of rows ranging from 301 to 201 to 151 to 61 on a side. There were always 301

columns. The model was run for 1 day. Analytical results for the five timesteps used in the model are presented in table 1. Two transmissivities were used to compare errors for values of large and small drawdown. Results for the model runs using the different combinations of cell dimensions and transmissivities are presented in table 2. Only the two extremes of cell dimensions are presented for a transmissivity of 5,000 ft²/d.

The results show that equation 4 gives very good results for estimating the analytical solution to the problem. For the lower value of transmissivity and square cell dimensions, equation 4 comes within 0.06 ft of the 26.35 ft of drawdown and the maximum error was 0.65 ft (0.02 percent) for a cell dimension of 500 by 100 ft. The error for the higher transmissivity was 0.00 for the square cell dimensions and 0.08 (0.03 percent) for the cell dimensions of 500 by 100 ft.

To confirm that the relation of the effective radius to cell dimension presented by Prickett (1967) is appropriate, the drawdown at the cell center was used in the Theis equation to calculate the appropriate analytical radius. For the cell dimensions of 100 by 100 and a transmissivity of 500 ft²/d, the analytical radius was 21.21 ft. The effective radius, r_e , from equation 1 was 20.79. The ratio of the effective radius to the analytical radius is 0.98 (20.79/21.21) whereas the ratio of the simulated drawdown to the analytical drawdown is 1.00 (26.29/26.35). For cell dimensions of 500 by 100 ft and a transmissivity of 500 ft²/d, the analytical radius was 76.55 ft and the effective radius was 62.37 ft. The ratio of the effective radius to the analytical radius was 0.81 (62.37/76.55) whereas the ratio of the simulated drawdown to the analytical drawdown was 0.97 (25.69/ 26.35). These results show that, although the error in effective radius may grow as the cell dimensions are exaggerated, the relative error in calculated head remains small. This result is not to say that cell dimensions are not

important. The cell dimensions tested were uniform in each direction. Care is still needed in a truly variable grid system where dimensions are being changed in each direction.

Table 1. Analytical results for pumping well used to test equation 4

Timestep	Time, in days	T = 500 ft ² /d			T = 5,000 ft ² /d		
		u	W(u)	s	u	W(u)	s
1	0.075829	6.59E ⁻⁷	13.6553	22.17	6.59E ⁻⁸	15.9579	2.59
2	0.189573	2.64E ⁻⁸	14.5703	23.65	2.64E ⁻⁸	16.8729	2.74
3	0.360190	1.39E ⁻⁷	15.2118	24.69	1.39E ⁻⁸	17.5144	2.84
4	0.616114	8.12E ⁻⁸	15.7491	25.57	8.12E ⁻⁹	18.0517	2.93
5	1.000000	5.00E ⁻⁸	16.2340	26.35	5.00E ⁻⁹	18.5366	3.01

Program Design

The program code consists of routines adapted from MODFLOW that provide the proper input of grid dimension, transmissivity data, pumping data, and output data. Program code from Trescott and others (1976) was added to calculate the head in a well. The output from the program lists much of the basic package information to identify the problem being modeled, output control flags for each timestep, and a table listing the well location, the head and drawdown in the well, and the radius of the well. If an actual head is available for the final timestep in a stress period, this head value and the difference between the actual and simulated heads will be printed. If starting heads are not saved (ISTRTR= 0), all drawdowns are set to zero in the tables.

Table 2. Comparison of analytical results to simulated results using equation 4 for varying grid dimensions and two values of transmissivity

	Head at time- step 1	Head at time- step 2	Head at time- step 3	Head at time- step 4	Head at time- step 5	Mass- balance error	Cell head, Time step 5	Draw down at boundary
Model with T = 500 ft ² /d								
Analytical	-22.17	-23.65	-24.69	-25.57	-26.35	----	----	----
100 x 100	-21.35	-23.35	-24.54	-25.47	-26.29	-0.07	16.44	0.00
150 x 100	-21.27	-23.28	-24.47	-25.41	-26.23	-0.07	15.65	0.00
200 x 100	-21.15	-23.17	-24.36	-25.30	-26.12	-0.06	14.95	0.00
500 x 100	-20.61	-22.70	-23.92	-24.87	-25.69	-0.06	12.27	0.00
Model with T = 5,000 ft ² /d								
Analytical	-2.59	-2.74	-2.84	-2.93	- 3.01			
100 x 100	-2.51	-2.71	-2.83	-2.92	-3.01	-0.51	2.02	0.06
500 x 100	-2.45	-2.65	-2.77	-2.86	-2.95	-0.31	1.61	0.06

The head in a pumping well (**hdpw**) code is designed to be a post-processor that may be executed by itself or within the same runfile as MODFLOW. If executed within the same runfile as MODFLOW, output tables may be written to the output listing of the modular model or to a separate file. The only changes to the MODFLOW input data is that a radius value is placed in columns 51-60 of the individual well record (record 3) for a head and drawdown to be calculated for a particular well and that a value of head for an actual measurement is placed in columns 61-70 for a comparison to be made between the calculated head and the measured head. If no radius is input (radius = 0), no calculation will be made for that well. If no actual head is input (ACHD=0), no comparison to the value of simulated head will be made. For a transient simulation, heads must be saved for each time period heads and drawdowns are to be calculated.

A general flow chart of the program is diagramed in figure 2. Data files for the MODFLOW modules of the BASIC, BLOCK-CENTERED FLOW, OUTPUT CONTROL, and WELL packages are read to provide input for the **hdpw** program. The basic package is read in its entirety to define the model dimensions and time parameters. The block-centered flow package has been truncated and modified to allow the transmissivity of grid cells to be calculated and stored. No aquifer coefficients (CC and CR) are calculated. The output control package is read in its entirety to mark times when heads are saved to disk. The time periods when heads are saved signals to the program that heads for wells will be calculated for

that time period. The well package is read in its entirety to define the wells that have finite radii and a subroutine (WELHPW) has been added to the MODFLOW well package that calculates the head and drawdown for a well.

Description of Subroutine WELHPW

The subroutine for calculating the head in a well (WELHPW) contains the following steps:

1. Reads unformatted record containing heads saved for appropriate time period.
2. Reads well records to determine if any wells have a finite radius.
3. For wells with a finite radius, computes effective radius for cell -- $r_e = (\text{DELCL}(I) + \text{DELCR}(J)) / 9.62$.
Note that the effective radius is calculated using the individual row and column lengths so the potential is there to place a well in a rectangular cell.
4. Determines if layer is under confined or unconfined conditions.
5. Uses appropriate equation to calculate head and drawdown in a well.
6. For wells with an actual head to compare for the end of a stress period, computes difference between actual head and simulated head.
7. Prints well location, well radius, and head and drawdown for the well at each timestep heads are saved and also prints actual head and the difference between actual and simulated heads for the final timestep of the stress period.

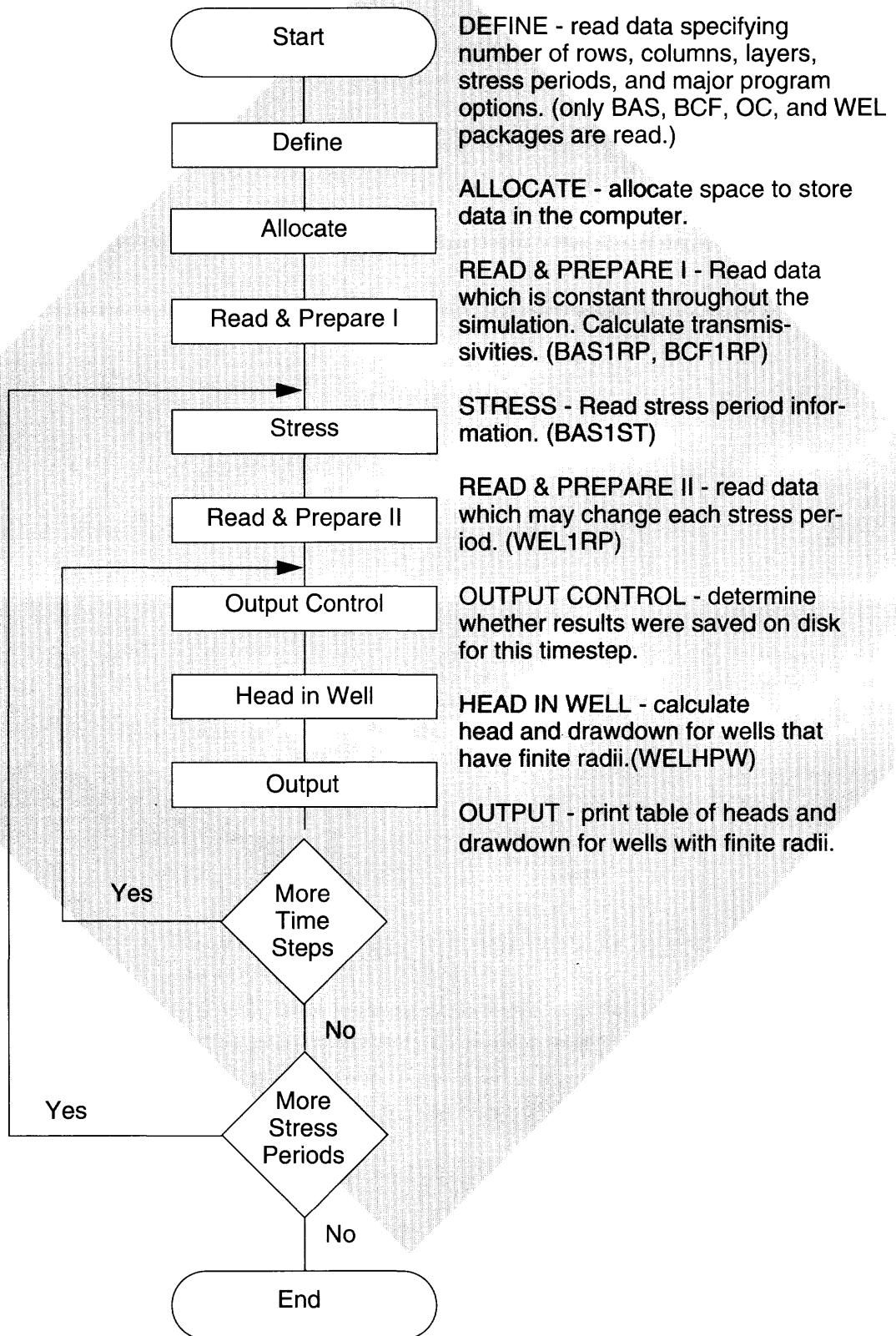


Figure 2. Program structure.

Input for Well Package

FOR EACH SIMULATION

WEL1AL		
1. Data:	MXWELL	IWELCB
Format:	I10	I10

FOR EACH STRESS PERIOD

WEL1RP							
2. Data:	ITMP						
Format:	I10						
3. Data:	Layer	Row	Column	Q	(IFACE)	R	ACHD
Format:	I10	I10	I10	F10.0	I10	F10.0	F10.0

MXWELL-- is the maximum number of wells used for any stress period.

IWELCB -- is a flag or unit number for cell-by-cell terms.

ITMP -- is the number of wells active during the present stress period.

Q -- is the discharge rate for the well. The rate is negative for a pumping well and positive for an injection well.

IFACE -- used in program MODPATH to designate faces of model cell used in determining flow rates. (Only needed if MODPATH is being used in analysis.)

R -- is the radius of the well.

ACHD -- is an actual (measured) head to be compared with the simulated head at the end of the stress period.

SAMPLE INPUT

Following is the input needed to run the post-processor **hdpw**.

Basic package

TEST OF HDPW AGAINST THEIRS ANALYTICAL SOLUTION --

ONE WELL PUMPING 53 GPM FOR T OF 500 SQFT/D.

```
          1          301          301          1          4
11 21 0 0 0 0 0 0 0 0 0 0 16 19 0 0 0 0 0 0 0 0
          0          0
          0          1          (40i2)          2
          0          0
          0          0          9
          1          5          1.5
```

Block-centered flow package

```
          0          62
0
          0          1
          0          100
          0          100
          0          .0001
          0          500
```

Output control package

```
          5          5          61          65
          1          1          1          62
          1          0          1          0
          1          1          1          62
          1          0          1          0
          1          1          1          62
          1          0          1          0
          1          1          1          62
          1          0          1          0
          1          1          1          62
          1          0          1          0
```

Well package

```
          1          62
          1
          1          151          151          -10200          6          1          -26.35
```

SAMPLE OUTPUT

```
*****
*****
U.S. GEOLOGICAL SURVEY HEAD IN A WELL OF FINITE RADIUS POST-PROCESSING PROGRAM
*****
*****
```

TEST OF HDPW AGAINST THEIS ANALYTICAL SOLUTION --
 ONE WELL PUMPING 53 GPM FOR T OF 500 SQFT/D.

1 LAYERS 301 ROWS 301 COLUMNS

1 STRESS PERIOD(S) IN SIMULATION

MODEL TIME UNIT IS DAYS

START HEAD WILL NOT BE SAVED -- DRAWDOWN CANNOT BE CALCULATED

816034 ELEMENTS OF X ARRAY USED OUT OF 1400000

WELL(S) IN CURRENT STRESS PERIOD = 1

LAYER	ROW	COL	STRESS RATE	RADIUS	HEAD	WELL NO.

1	151	151	-10200.	1.0000	-26.350	1

```
*****
OUTPUT FLAGS FOR EACH LAYER:
```

LAYER	HEAD PRINTOUT	DRAWDOWN PRINTOUT	HEAD SAVE	DRAWDOWN SAVE

1	1	0	1	0

HEAD AND DRAWDOWN IN PUMPING WELLS FOR STRESS PERIOD 1, TIMESTEP 1
 TIME SIMULATED = 0.7582939E-01

I	J	K	WELL RADIUS	HEAD	DRAWDOWN

151	151	1	1.00	-21.35	0.00

OUTPUT FLAGS FOR EACH LAYER:

LAYER	HEAD PRINTOUT	DRAWDOWN PRINTOUT	HEAD SAVE	DRAWDOWN SAVE
1	1	0	1	0

HEAD AND DRAWDOWN IN PUMPING WELLS FOR STRESS PERIOD 1, TIMESTEP 2
 TIME SIMULATED = 0.1895735

I	J	K	WELL RADIUS	HEAD	DRAWDOWN
151	151	1	1.00	-23.35	0.00

OUTPUT FLAGS FOR EACH LAYER:

LAYER	HEAD PRINTOUT	DRAWDOWN PRINTOUT	HEAD SAVE	DRAWDOWN SAVE
1	1	0	1	0

HEAD AND DRAWDOWN IN PUMPING WELLS FOR STRESS PERIOD 1, TIMESTEP 3
 TIME SIMULATED = 0.3601896

I	J	K	WELL RADIUS	HEAD	DRAWDOWN
151	151	1	1.00	-24.54	0.00

OUTPUT FLAGS FOR EACH LAYER:

LAYER	HEAD PRINTOUT	DRAWDOWN PRINTOUT	HEAD SAVE	DRAWDOWN SAVE
1	1	0	1	0

HEAD AND DRAWDOWN IN PUMPING WELLS FOR STRESS PERIOD 1, TIMESTEP 4
 TIME SIMULATED = 0.6161138

I	J	K	WELL RADIUS	HEAD	DRAWDOWN
151	151	1	1.00	-25.47	0.00

OUTPUT FLAGS FOR EACH LAYER:

LAYER	HEAD PRINTOUT	DRAWDOWN PRINTOUT	HEAD SAVE	DRAWDOWN SAVE
1	1	0	1	0

HEAD AND DRAWDOWN IN PUMPING WELLS FOR STRESS PERIOD 1, TIMESTEP 5
 TIME SIMULATED = 1.000000

I	J	K	WELL RADIUS	HEAD	DRAWDOWN	ACTUAL HEAD	DIFFERENCE
151	151	1	1.00	-26.29	0.00	-26.35	0.06

REFERENCES

- Akbar, A.M., Arnold, M.D., and Harvey, O.H., 1974, Numerical simulation of individual wells in a field simulation model: Society of Petroleum Engineers Journal, August, p. 315-320.
- McDonald, M.G., and Harbaugh, A.W., 1988, A modular three-dimensional finite-difference ground-water flow model: U.S. Geological Survey Techniques of Water-Resources Investigations, book 6, chap. A1, 586 p.
- Prickett, T.A., 1967, Designing pumped well characteristics into electric analog models: Ground Water, v. 5, no. 4, p. 38-46.
- Prickett, T.A., and Lonquist, C.G., 1971, Selected digital computer techniques for groundwater resources evaluation: Illinois State Water Survey Bulletin 55, 62 p.
- Theis, C.V., 1935, The relationship between the lowering of the piezometric surface and the rate and duration of discharge of a well using groundwater storage: American Geophysical Union Transaction, v.16, p. 519-524.
- Thiem, Gunther, 1906, Hydrologische Methoden: Leipzig, J.M. Gebhardt, 56 p.
- Trescott, P.C., Pinder, G.F., and Larson, S.P., 1976, Finite-difference model for aquifer simulation in two dimensions with results of numerical experiments: U.S. Geological Survey Techniques of Water-Resources Investigations, book 7, chap. C1, 116 p.